DEVELOPMENT OF CORRELATION FOR THERMOPHYSICAL PROPERTIES OF SUPERCRITICAL ARGON TO BE USED IN FUTURISTIC HTS CABLES

M.Tech Dissertation

By

Mohit Kalsia

(11301079)

DEPARTMENT OF MECHANICAL ENGINEERING

LOVELY PROFESSIONAL UNIVERSITY

PHAGWARA, PUNJAB (INDIA) -144411

2014- 2015

DEVELOPMENT OF CORRELATION FOR THERMOPHYSICAL PROPERTIES OF SUPERCRITICAL ARGON TO BE USED IN FUTURISTIC HTS CABLES

DISSERTATION-II

Submitted in Partial Fulfilment of the

Requirement for Award of the Degree

Of

MASTER OF TECHNOLOGY

In

MECHANICAL ENGINEERING

By

MOHIT KALSIA

(11300829)

Under the Guidance of

Mr RAJA SEKHAR DONDAPATI

DEPARTMENT OF MECHANICAL ENGINEERING

LOVELY PROFESSIONAL UNIVERSITY

PHAGWARA,

PUNJAB (INDIA) -144411

(2014-15)

Lovely Professional University, Jalandhar, Punjab

CERTIFICATE

I hereby certify that the work which is being presented in the dissertation entitled **"Development of Correlation for Thermophysical Properties of Supercritical Argon to be used in futuristic HTS Cables"** in partial fulfilment of the requirement for the award of degree of **Master of Technology** and submitted in Department of Mechanical Engineering, Lovely Professional University, Punjab is an authentic record of my own work carried out during period of Dissertation under the supervision of **Mr Raja Sekhar Dondapati**, **Assistant Professor**, Department of Mechanical Engineering, Lovely Professional University, Punjab.

The matter presented in this dissertation has not been submitted by me anywhere for the award of any other degree or to any other institute.

Date: **Mohit Kalsia**

This is to certify that the above statement made by the candidate is correct to best of my knowledge.

Date: **Mr Raja Sekhar Dondapati**
Supervisor

The M- Tech Dissertation examination of Syed Mahaboob Idris, has been held on _____

Signature of Examiner

ACKNOWLEDGEMENT

I am deeply indebted to my dissertation advisors, Assist Prof. Raja Sekhar Dondapati, Assist Prof. Gaurav Vyas for their respectable guidance, support and encouragement. This dissertation would not have been accomplished without their valuable advices and thoughts.

I am grateful to Mrs Preeti Rao Usurumarti for her guidance during my whole dissertation work. I would like to thank to Dr. Rajiv Kumar Sharma (Head of Thermal Engineering Department), Dr. Amit (Head of Manufacturing Department) and Mr Gurpreet Singh Phull (Head of Design Engineering Department) for their priceless support.

I would also like to thank Mr Barjinder Singh Bedi, Mr. Ankur Bahl, Mr. Dilbaj Singh, Mr. Minesh Vohra, Mr. Aashish Sharma, Ms. Garima, Mr. Varun Goyal, Mr. Harpal Singh, Mr. P. Narasimha Vinod, Mr. Pyuesh Gulati, Mr. Ankit Sharma and Mr Vijay Shankar for their intense support in developing my thesis to the present stage.

I am also grateful to my research team members Mr. Jeswanth Ravula, Mr. Aal Arif Sarkar, Mr. Syed Mahaboob Idris, Mr. Shivam S Verma, Mr. Ajay Kumar Ramani, Mr. S. Mugilan, Mr.U. Venkataramana, Mr .G. Rajesh, Mr. Balakrishna pandian who have helped me during my short period of association with them and friends Mr. Sumit Saini, Mr. B.Pavan Kumar who indirectly supported gave their valuable support and suggestions.

Last but not the least, my special gratitude and love go to my parents for their endless love, support and encouragement throughout my life. Acknowledging the parents support would be the foremost in achieving what I am now.

Mohit Kalsia

NOMENCLATURE

P	Pressure
P_c	Critical Pressure
T	Temperature
T_c	Critical Temperature
H	Magnetic Field
H_c	Critical Magnetic Field
HTS	High Temperature Superconductor
TWh	Tera Watt Hour
SCAR	Super Critical Argon
LTS	Low Temperature Superconductor
SCFs	Super-critical Fluids
P-V-T	Pressure-Volume-Temperature
SS316LN	Stainless steel pipe
DC	Direct current
AC	Alternative Current
NIST	National Institute of Standard and Technology
REFROP	REFrigerant PROPerties software program
LN2	Liquid Nitrogen
CFD	Computational Fluid Dynamics
Cu	Copper
MVA	Mega Volt Ampere
Ag/Bi-2223	Silver/Bismuth-2223
YBCO	Yttrium Barium Cooper Oxide

BSCCO	Barium Strontium Calcium Cooper Oxide
MPa	Mega- Pascal
NMR	Nuclear Magnetic Resonance
AARE	Average Absolute Relative Error
PRE	Percent Relative Error

ABSTRACT

Most of the power transmission systems are to be replaced by high temperature superconducting (HTS) cables for efficient operation. These HTS cables need to be cooled below the critical temperature of superconductors used in constructing the cable. With the advent of new superconductors whose critical temperatures having reached up to 134K (Hg based), need arises to find a suitable coolant which can accommodate the heating load on the superconductors. In order to accomplish such challenge an attempt has been made in the present work to identify suitable Thermophysical properties of supercritical argon (SCAR). The Thermophysical properties such as density, viscosity, specific heat and thermal conductivity of SCAR found to be drastically varying with respect to temperature at a particular pressure. Moreover, it is observed that with an increase in pressure density and viscosity are increasing. In addition, as the temperature increases a shift in Thermophysical properties is observed. Few correlations are developed which are applicable over a wide range of temperatures. These correlations may be useful in thermohydraulic modeling of HTS cables using numerical or computational techniques. In recent times, with the sophistication of computer technology, solving of various transport equations with temperature dependent thermophysical properties became popular and hence the developed correlations would benefit the technological community.

Keywords: Supercritical Argon, HTS Cables, Correlations

CHAPTER

1 INTRODUCTION

1.1 BACKGROUND

Energy has been entirely acknowledged as the most important factor for economy and human development of any nation. A rapid increase in the population rate results, instant increase in consumption of energy. Since, energy exists in various forms in the nature but the most dominant form is the electrical energy. Electrical energy has taken a lead role in our life due to the more dependency of modern world on it.

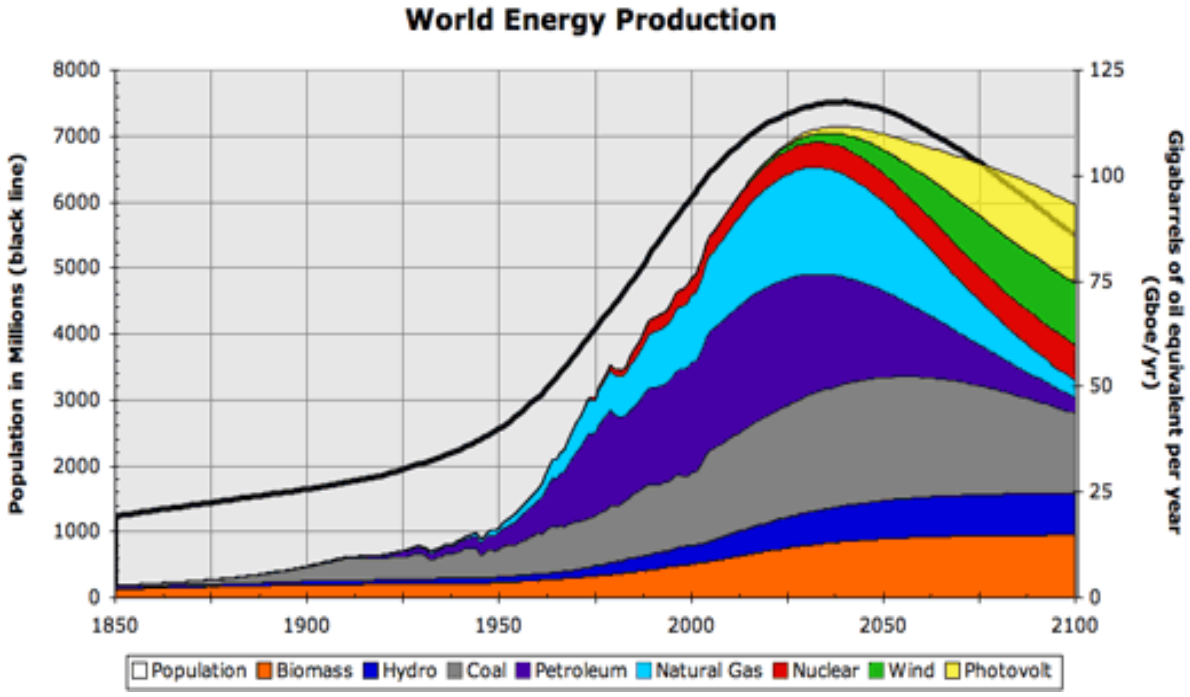

Figure 0-1 World energy production versus consumption

(Source: http://www.iceuls.com/_photo/b.jpg)

This figure shows the production rate of energy by various sources throughout the world. Since, electrical energy is produced by the use of available forms in nature such as Biomass, Hydro, Petroleum, Natural gas, Nuclear, coal and Wind etc. Using these sources, (TW-h) tera watt hour of energy being produced all over the world through power plants for the different purposes such as commercial, industrial and domestic. However, this large quantity of produced electric energy (TW-h) tera watt hour is wasted about (50-60) % to

the environment while transmitted through transmission lines using normal conductors. Furthermore, while high current flow through the conventional cables, it withstands more energy losses such as eddy current or hysteresis (cable core), dielectric loss, current resistivity and heat leakage in insulation.

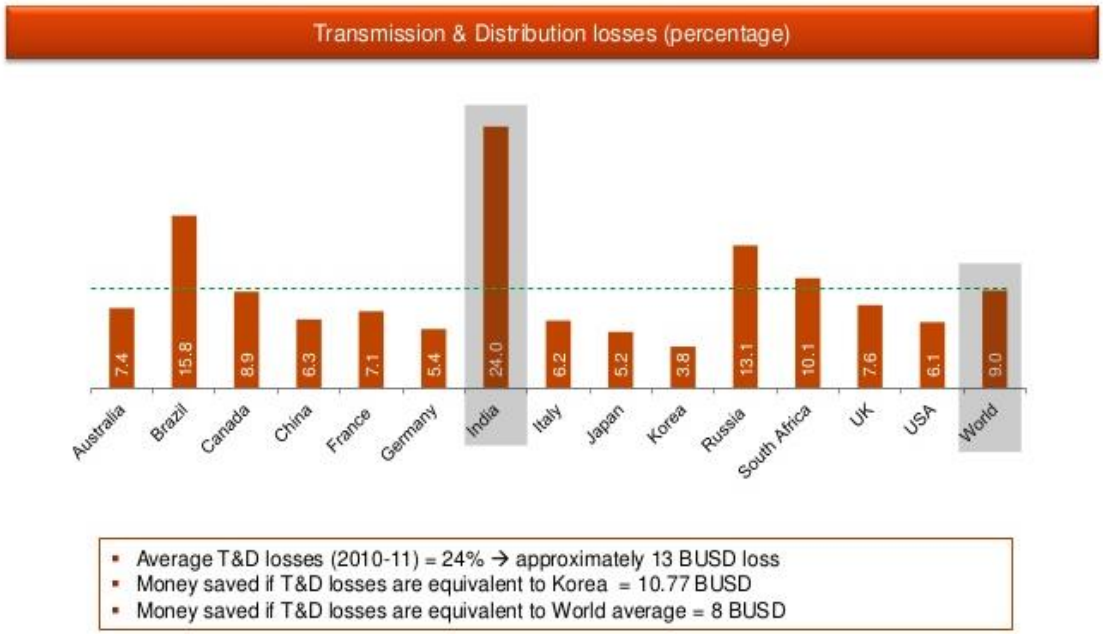

Figure 0-2 Transmission and distribution losses

(Source: http://image.slidesharecdn.com)

This figure illustrates the losses during transmission and distribution of electric energy through the conventional cables around whole of the world. In order to overcome all these losses and 100% efficient transmission of electric energy (electricity), conventional cables has to be replaced by HTS (high temperature superconducting) cables. Therefore, to accomplish the challenge of losses to be negligible, various communities has been developing the HTS (High Temperature Superconducting) cables as the solution of problem discussed earlier.

Thus, in this present scenario, High Temperature Superconductors are widely used in different applications such as generators, storage devices, transmission cables, and transformers etc. Due to the increasing demand and supply of energy with high capacity and small underground space, HTS cables are emerging as a solution of power transmission with high efficiency, reduced heat generation, lower weight and high current carrying capacity. Furthermore, thousands of megawatt of electric power produced by generators could be transmitted without any losses and environmental issues. However,

these cables require attention with regard to design, manufacturing [1-2], laying and safe operation. In order to safely operate these HTS cables, efficient cooling methodologies must be employed with judicious selection of coolant. Supercritical fluids, due to their peculiar properties, may be employed in cooling HTS cables.

Figure 3 Geometry of HTS coaxial cable with cold dielectric configuration modelled using ABAQUS [10]

Thermophysical properties, such as density, viscosity, thermal conductivity, specific heat and other properties vary significantly as the pressure and temperature of fluid exceeds above the critical values. HTS cable with single layer of HTS tapes is shown in Figure 3. In this context, it is important to consider the properties of superconducting materials, sheath materials, former material, dielectric materials, electrical shielding, thermal insulators and properties of coolants at cryogenic temperatures while designing of the HTS cables. The properties of each material stated above at cryogenic temperatures vary considerably and depend on the operating temperature (T_o). These issues necessitate the study of thermophysical properties applicable to the design of HTS cables. Since, HTS cables are based on the principle of superconductivity, which will be discussed below.

CHAPTER

2 TERMONOLOGY

2.1. SUPERCONDUCTIVITY

The phenomenon of losing resistivity and expulsion of magnetic field, when cooled to a certain temperature (below critical temperature, T_c). Superconductivity is discovered by Dutch Physicist Heike Kamerlingh Onnes on April 8, 1911 in Leiden.

Critical Temperature (T_c) - Temperature at which a normal conductor loses its resistivity and becomes a superconductor.

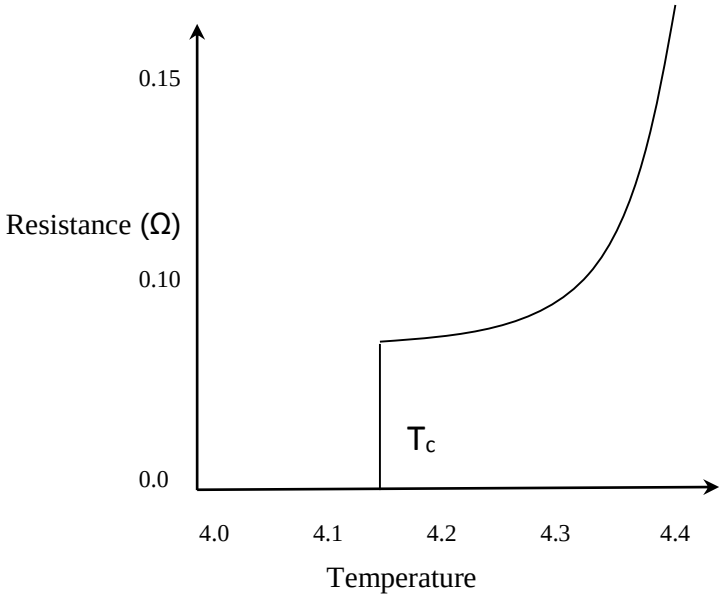

Figure 2-1 superconducting phenomenon of mercury

The above diagram indicates that the resistivity would be exactly zero at the critical temperature (T_c) for a superconductor. In this figure, mercury (Hg) has taken into consideration having critical temperature nearer to 4K, mercury was developed as the first superconducting substance.

Because this metal offered the best conditions for the study of intrinsic properties of metals at low temperatures due to the purity at which it could be obtained. At the time of discovery and even today purity is indeed a valid consideration, when studying electrical conductivity versus temperature.

In addition, to define the critical surface where the superconducting phase can exist, two other parameters such as critical field *Hc* and critical current density *Jc* are required to be considered. Whereas, for a given superconducting material *Tc* and *Hc* are considered as thermodynamic properties.

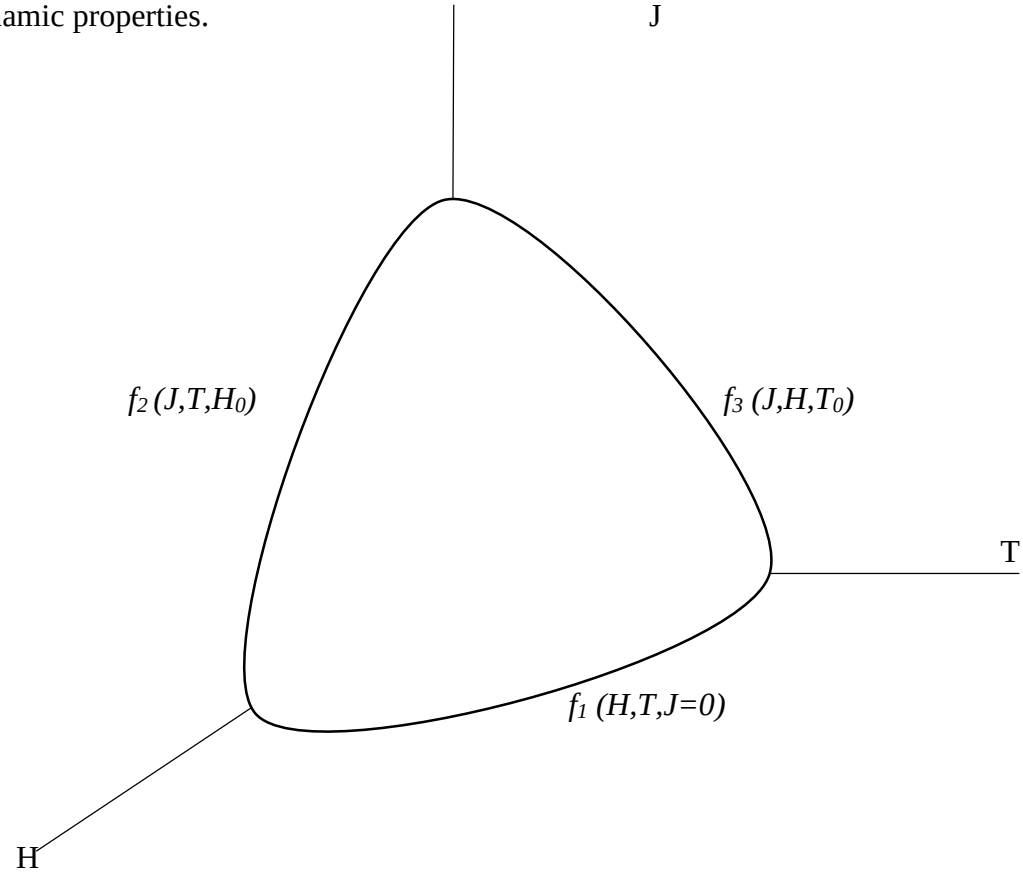

Figure 2-2 Critical surface of a magnet-grade superconductor.

The critical surface for a magnet-grade superconductor is shown in this figure. The various three important parameters are used on this critical surface: f_1 (H,T,J = 0); f_2 (J,T,H o=constant); f_3 (J,H,T_o =constant). Where f_1 is the plot between H_c & T_c, f_2 is plot between J_c & T_c and plot between J_c & H_c represents f_3.

Superconductivity is classified by meissner effect i.e. the complete expulsion of magnetic lines from inside of superconductors.

Figure 2-3 Meissner Effect

(Source: http://www.childzgraphicdesign.com/)

Figure 4 shows that when superconductor is to be placed in magnetic field under the condition ($T<T_c$), it excludes the magnetic field. This phenomenon was discovered by German Physicists Walther Meissner and Robert Ochsenfeld in 1933.

Thus, while passing the current into a superconductor, its electrical resistivity decreases gradually or becomes zero until it will be in superconducting state. Therefore, to maintain the superconductivity of the superconductor, **Cryogenics** emerge as a solution.

Cryogenics plays a vital role in maintaining the superconductivity of superconductor. The basic concept of Cryogenic that it deals with low temperature, (<123K, -150^{o}C). Gases (such as helium, hydrogen, neon, nitrogen, and oxygen) lie below −180 °C comes under cryogenics fluid. Some liquefied gases, such as liquid nitrogen and liquid helium, are widely used in many cryogenic applications due to their easy availability and purchasability around the world. These liquids can be stored in Dewar flasks, which are double-walled containers with a high vacuum between the walls to reduce heat transfer into the liquid. Usually, liquid nitrogen is used as cryogenic coolant in HTS applications due to the easy availability of nitrogen in ambient air.

2.2. History of Superconductors

Superconductors are categorized mainly in two parts:

1) Type 1 Superconductor
2) Type 2 Superconductor

Type 1 Superconductors:

It consist generally soft superconductors, in which magnetisation loss occurs suddenly and exhibit meissner effect. E.g. Pb, Hg, Sn. Due to the low H_c values i.e. ($<10^5$ A/m~0.1 T) Type I superconductors, are unsuitable as magnet conductor materials.

Type 2 Superconductors:

Hard superconductors with gradual magnetisation losses and does not exhibit meissner effect. E.g. Nb-Ti, Nb-Sn. A Type II superconductor may be modeled as a finely divided mixture of a Type I superconductor and normal conducting material.

Superconductors are formed into two types

1. Low temperature superconductors (T_c <30K).
2. High temperature superconductors (T_c >30K).

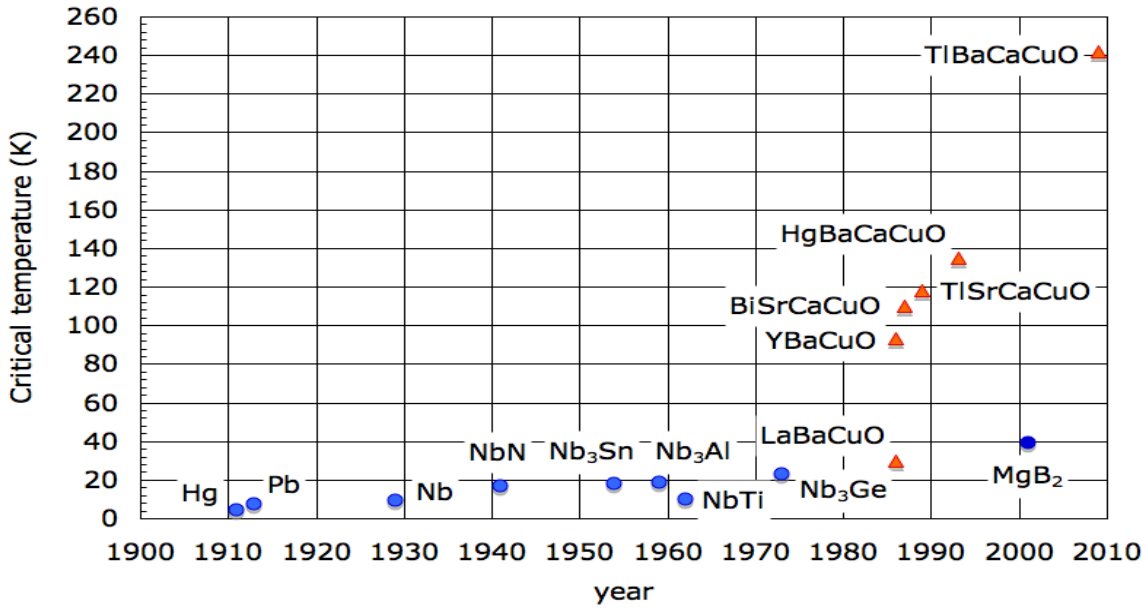

Figure 2-4 History of superconductors

(Source: www.ccas-web.org)

This figure shows that the discovery of superconductors has been started from 1911 and in this decade of time (1911 to 1986), all the low temperature superconductors (T_c<23K) has been founded. Thus, after these revolutionary years, first high temperature superconductor (LaBaCuo) has discovered in January 1986 having critical temperature of 35K. Similarly, the discovery of high temperature superconductors has been started and not ended yet. Nowadays (BiSrCaCuO) T_c =110K, as high temperature superconductor is in used for designing the HTS cable. The other high temperature superconductors such as (Tl-Ba-Ca-Cu-O) T_c =125K and (Hg-Ba-Ca-Cu-O) T_c =133K has been discovered however, the manufacturing of these high temperature superconductors is under process. Therefore, the aim of researchers that to find a room temperature superconductor (T_c=300K), so that the requirement of cryogenic fluid which needs to maintain the superconductivity of superconductor could be less.

2.3. APPLICATIONS OF SUPERCONDUCTORS

Superconductors are having huge application field due to its some unique properties like zero resistance to DC, very high current carrying density, tremendously low resistance at high frequencies, very low signal dispersion, Great sensitivity to magnetic field, Segregation of applied magnetic field, Quick single flux quantum transfer, Close to speed of light signal transmission and more. Nowadays, superconductors are having a great impact in different fields such as:

a. Electric power application

HTS wires system

Installed HTS system

b. Transportation application,

Superconductors are enabling a new generation of transport technologies including ship propulsion systems, magnetically levitated trains,

A view of Levitating trains

c. Medical Imaging and Diagnostics,

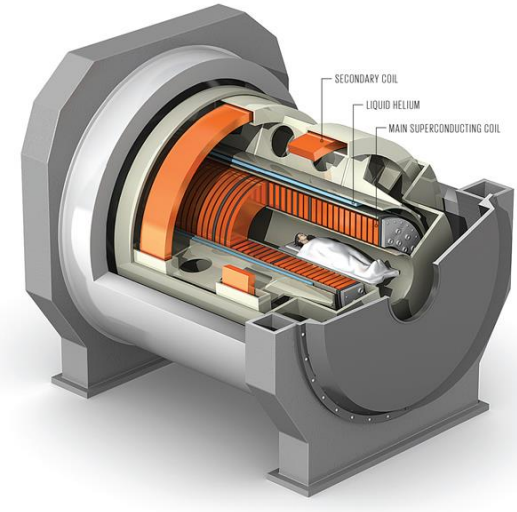

Superconducting MRI system in operation

An example of an MRI brain scan

d. Pharmaceuticals,

NMR (Nuclear Magnetic Resonance), is the critical tool for genomics, drug discovery, and biotechnology. LTS materials allow the stable and homogeneous magnets required for precision NMR spectroscopy.

e. Biotechnology,

f. Genomics and Materials Science,
g. Industrial processing,
h. wireless communications,
i. Instrumentation and Sensors,
j. Standards and Radar

With lot many great application field of Superconductors, there are some challenges which cannot be ignored. These challenges are as follows:

a. Cost
b. Refrigeration
c. Reliability
d. Acceptance

2.4. HTS POWER CABLE

The HTS power cable consists some important parts are shown above in figure 3.

a. Corrugated steel pipe
b. HTS Tape
c. Thermal insulation
d. Dielectric
e. Cable Shield

CORRUGATED STEEL PIPE: This corrugated pipe is made up of Stainless steel SS316 and its main purpose is to provide the flexibility to complete HTS cable while installing it underground and having curvature.

HTS TAPE: HTS tapes are the main part of HTS cables, through which flow of current takes place. There are two types of tapes are to be found i.e. Bismuth Strontium calcium copper oxide (BSSCO) which is first generations HTS tape having critical temperature 110K. On the other hand Yttrium Barium Copper oxide (YBCO) which is second generation HTS tape having critical Temperature 90K. As per the diameter of former/corrugated pipe, the number of tapes is required or can be calculated. The HTS tape is having <0.1 mm thickness.

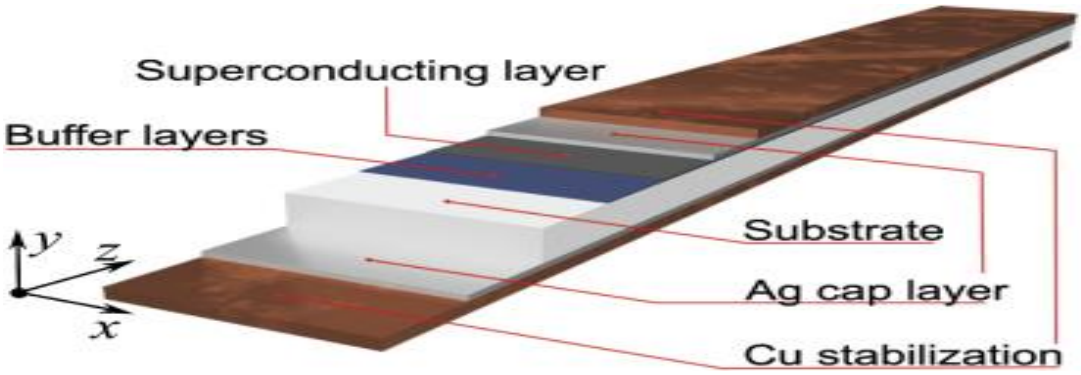

Figure 2-5 General View of HTS Tape

(Source: http://iopscience.iop.org)

THERMAL INSULATION: Under vacuum conditions, thermal simulation is used to create a heat barrier or to protect heat leaking from the ambient. Few thermal insulters are available such as Polyamide and foam.

2.5. SUPERCRITICAL FLUIDS

Supercritical fluid (SCFs) was discovered by Baron Charles Cagniard de La Tour In 1822. A supercritical fluid is any substance at a temperature and pressure above its critical point (**Error! Reference source not found.**). And at critical point, distinct liquid and gas phases do not exist. Supercritical fluids consist of both liquid and gases properties and it form a new state of matter.

At the critical point, the gas-liquid interface disappears and the fluid exhibits unique transport and thermodynamic properties. These properties like densities, which leads to significant increase in solubility, gas-like diffusivities, viscosities and also zero surface tensions which further benefits in mass transfer and fluid mixing. The formed new state of fluid is highly compressible than the liquid phase therefore density becomes a strong variable of both temperature and pressure which leads to adding more complexion in order to understand the flow behaviour and reaction mechanism for practical models.

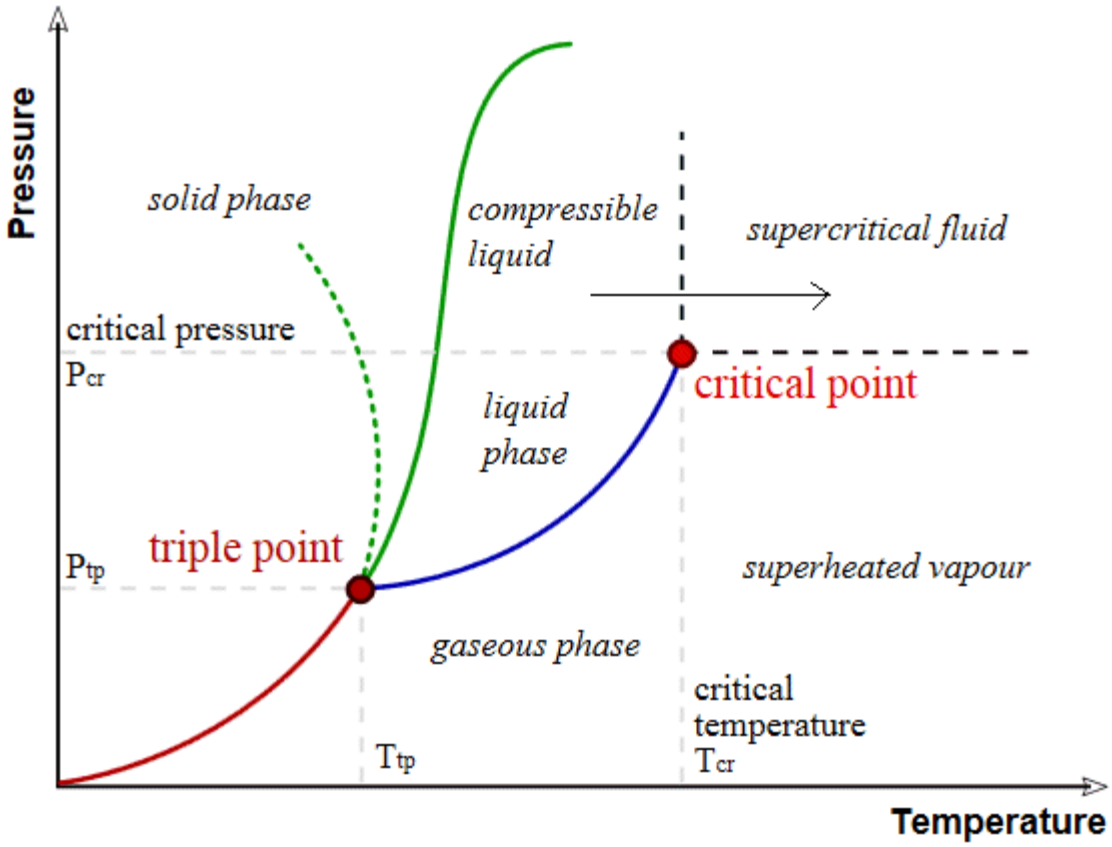

Figure 2-6 A typical P-T phase diagram of a pure substance.

(Source: www.intechopen.com)

Some facts about Supercritical Fluids

a) Any small changes in pressure or temperature nearer to critical point, results in large variations in thermodynamic properties like densities. Thus, by changing temperature or pressure of the fluid, the properties can be "tuned" to be more liquid or more gas-like as per requirements.
b) Impossible to liquefy the matter using any amount of pressure due to high density and low viscosities of supercritical fluid.
c) Solubility, at constant temperature, in a supercritical fluid tends to increase with density of fluid. Since density tends to increase with pressure which leads to increase in solubility also. Solubility tends to increase with temperature, at constant density.

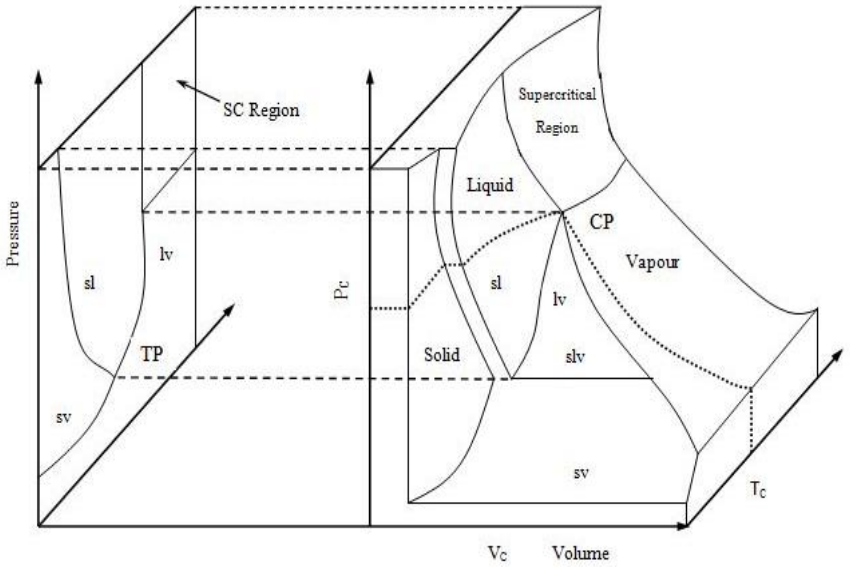

Figure 2-7 P-V-T diagram of a pure substance and its projection on the P-T plane.

The different physical states of pure substance can be visualized in a 3-D pressure-volume-temperature (P-V-T) diagram as shown in Figure 2-8.

As per Gibbs phase rule, if a pure substance exists in two phases (solid-liquid, solid-vapour and liquid-vapour), then there is only one degree of freedom. Thus, the equilibrium pressure in each case will be a function of temperature only. In P-V-T diagram, the vapour-liquid line represents the vapour pressure curve that starts from triple point (TP) and ends at the critical point (CP). As the temperature increases, the density of liquid phase diminishes and vapour density increases due to the higher vapour pressure. Above the critical point, as both the densities converges at the critical point and it becomes no longer possible to differentiate the liquid or vapour states. A rough idea about the property difference between the SCF and liquid fuel is given in **Error! Reference source not found.**. SCFs bring new directions to diesel fuel combustion research due to their unique properties.

Table 2-1 Comparison of the physical properties of gas, liquid and supercritical fluids .

Physical Property	Gas ($T_{ambient}$)	SCF (T_C, P_C)	Liquid ($T_{ambient}$)
Density (kg/m^3)	0.6-2	200-500	600-1600
Dynamic viscosity (µPa-s)	0.01-0.3	0.01-0.03	0.2-3
Thermal conductivity (W/m-K)	0.01-0.025	Maximum	0.1-0.2
Surface tension (dyn/cm^2)	-	-	20-40

CHAPTER

3 LITERATURE REVIEW

3.1. INTRODUCTION

The concepts related to the proposed work reviewed in this literature review such as designing, fabrication, evaluation of HTS cable power system. Correlations for thermophysical properties of supercritical fluid (Argoon) was reviewed. Few previous results from different Authors studies have been studied in this review.

Studies based on design and manufacturing part of HTS cable

Design of superconducting power cables: [1]

The design studies show that for 500MW class superconducting power cables with warm dielectrics, a line voltage of 110 KV seems to be reasonable. The minimum achievable losses strongly depend on the inner radius of phase conductor (r_{isc}). By taking care of conductor cost and resulting losses, an optimum operating temperature just below 60K has been found for Bi-2223. The low-cost Bi-2212 (operating temperature 50K) could be an alternative to the Bi-2223. Clearly, it is observed that superconducting cables would become economically competitive with conventional power cables only for the low conductor cost. Therefore the minimum rated power for high critical temperature cables allowing economic operation is expected to be as low as 500 MW.

Manufacture and Insulating Test of a Mini-Model for 154 kV-Class HTS Cables: [2]
Present work designates regarding the cables core design, electricity insulation design and pressure effect on insulation characteristics. The study concluded that, the 154 KV HTS cables has the highest voltage level in the world is being developed by research and development part in Korea. Further, study investigates as pressure increases of liquid nitrogen (LN_2), improves the insulation force. The thickness of the insulation layer which can be calculated by $t = r_c * [(\exp V_{ac} / E_{\max} * r_c) - 1]$, when thickness of LPP is 100 μm, 125 μm, 170 μm respectively. By, using mini-model cables, the bending test states that the insulation characteristics decline until no. of bending is 4 times, and afterward there is no change under the condition $R / r = 25$. So, 1.3 to 1.5 of design margins should be considered in determining thickness of the insulation for the same insulation characteristics of straight mini-model cable.

A novel correlation approach to estimate thermal conductivity of pure carbon dioxide in the supercritical region: [3]

In the absence of experimental measurements, an efficient numerical model for calculating the thermal conductivity has been presented in the current study. Within the valid temperature range 310K to 910K and pressure range between 7.4 to 210 Mpa from 668 experimental measurements, this model was derived. Less AARE% value 2.7 and 2.4 respectively is to be observed in comparison with literature experimental data and NIST data. The statistical parameter specifies the simple and superior model than others and needed less no. of complicated computations and parameters. Therefore the correlation founded in this work is $\lambda = \frac{A_1 + A_2 p + A_3 \rho^2 + A_4 \ln T + A_5 \ln T^2}{1 + A_6 P + A_2 \ln T + A_8 \ln T^2 + A_9 \ln T^3}$

A simple correlation to predict thermal conductivity of supercritical carbon dioxide [4]

To calculate accurately the thermal conductivity of CO_2 as function of temperature and density, an informal correlation has been proposed in this present work. The correlation is to find the thermal conductivity of CO_2, $\lambda = \frac{A_1 + A_2 \rho + A_3 \rho^2 + A_4 \rho^3 T^3 + A_5 \rho^4 + A_6 T + A_7 T^2}{\sqrt{T}}$

The main advantage of the correlation to be found is that no need of large parameters and complicated computation. It is obtained that the thermal conductivity of supercritical carbon dioxide for density and temperatures ranges between 1 to 1200 kg / m^3 and 290 to 800K respectively. Minimum value of AARE% showed the result of thermal conductivity correlation. In future the correlation helps in mathematical modeling of real system in the design of chemical engineering processes and in gas industries.

Flow and heat transfer characteristics of supercritical nitrogen in a vertical mini-tube: [5]

The experimental and numerical study of fluid flow and heat transfer characteristics of supercritical Nitrogen in the mini tube of dia. 2.0mm is being studied in the present work. During the investigation it is to be found that the variation of the thermal properties and buoyancy force affects the heat transfer. Correlation by Dittus – Boelter and yoon et al. can only predict the general trend of nusselt number and discrepancy between results due to the effect of buoyancy force. As temperature changes significantly the frictional pressure drop first increases and then decreases, also influenced by variation of thermal properties. The

overall agreements for the heat transfer coefficient and the pressure drop are about 35% and 25%, respectively, which shows that the numerical analysis procedure is potentially applicable to the flow and heat transfer analysis for the CICCs magnet cooling.

Design of HTS Tape Characteristics Measurement System: [6]

To measure the (I_c) critical current and AC losses, a measurement system has developed in this proposed work. In addition, to investigate the characteristics of the HTS tapes in a more practical environment with magnetic field and mechanical stress, this system can used. Moreover, the HTS tapes are under mechanical load at the same time, as well as bending, tension or twisting are considered in this present work. This system can be used to measure magnetization loss, if the pick-up coil and cancel coil were developed. The more research work is going on this field.

A Design and Tests of HTS Power Cables and Feasibility Study of HTS Power Transmission System in KOREA: [7]

In this present study, after evaluation of the prototype HTS cables, DC critical current of 730A has been achieved. Moreover, it is observed that about 50.4% decrease in cable Ic in inner layer when current passed through the total cable and 60% decreased when current passed through outer layer alone as compared to short sample Ic. The self-field is expected to be dominant degradation factor in cable configuration, among all the decreasing reasons. Furthermore, it can be observed that about 5% to 9.7% underground line would be reduced by HTS power cable, as compared to normal system in seoul. Eventually, after testing, evaluation the results have offered valuable data for the development of HTS cable. This amount of work has been done in this proposed work and in future a 3m cable of 1000A, 30 KV, with cryogenic insulation and cooling system will be constructed and tested the AC characteristics.

Calculation of Alternating Current Distribution on the Current Lead for HTS Power Cable: [8]

To design the current lead for HTS cables termination, AC has been considered as an important parameter. Due to the term (skin effect) the current were distributed on the edge of the current lead, when AC were flowing on current lead and result in non-uniformity of current density across the cross-section of current lead. With increase in the area, the influence of skin effect became serious and therefore heat load on AC current lead

increased. It can be observed that higher heat loads were generated in AC current leads compared to DC current leads due to the skin effect. The heat load increased about 15% compared to DC current lead, when AC of 1260amp were flowing in AC current lead with radius of 25 mm and length of 1.5m. To overcome the non-uniformity and AC loss produced due to skin effect, AC current lead has divided into some current leads had smaller cross-sections than the original current lead. In this case mutual inductance was found to be important. AC loss and current increased due to impact of mutual inductance, as the current leads were arrayed with a finite gap distance. In order to reduce these increments the twisting of divided current leads has been considered as or acted as like single current lead.

Modified Redlich–Kwong equation of state for supercritical carbon dioxide: [9]

A further proficient modification of the van der Waals equation by introducing temperature dependence has been stated in present work for determining the density of carbon dioxide through Redlich- Kwong. Minimum value of AARE% i.e. 1.63 and 2.07% in comparison with the literature experimental data and NIST data has resulted in this proposed modified work. The modification is considered based on 3742 experimental data point and is valid in the super critical region. The model is simple and does not need to a large number of parameters and complicated computations.

Pressure Drop and Heat Transfer Analysis of Long Length Internally Cooled HTS Cables. [10]

Some interesting facts on the velocity and temperature distribution in HTS cable are revealed by pressure drop and heat transfer analysis in HTS cables. The phenomenon of turbulence promotion and enhancement of heat transfer in HTS cables also explains in this analysis. At constant corrugation depth, the pressure drop increases and heat transfer rate also increases with the increase in corrugation pitch that can be concluded from this analysis. In order to increase the heat transfer further, twisted tapes may be inserted in the path of the coolant, thereby promoting the turbulence. A marginal pressure drop may be expected by the insertion of twisted tapes. However, some studies in this direction would help in enhancing the heat transfer rate significantly with minimum penalty of pressure drop.

A. Sasaki, LN2 circulation in cryopipes of superconducting power transmission line, [11]

In this work, the high temperature superconductors has used in application of superconducting power transmission lines (SC PTs) to reduce electricity losses using LN_2 as coolant. To calculate the pressure drop along the lengths of bellow pipes and straight pipes, empirical and CFD method is used in the present work. Using empirical formula pressure drop for long pipes can be calculated, and for decentering bellow pipes CFD method has used with short length due to the complexity in mesh generation and computational time. Moreover, pumping power and circulation losses are also estimated using both the methods. In CFD method realizable k-ϵ turbulent model is being used to get approximate results. In this study Author has concluded that for 10 km of cable length 10w of pumping power and 15kg/s of flow rate is required.

J. Fang , Numerical analysis of the stability of HTS power cable under fault current considering the gaps in the cable [12]

In this study, at the fault current 25 kA@3 s, the equivalent circuit model of HTS cable was established. Four conductor layers such as a copper cryopipe (Cu), HTS conductor layers, electrical insulation layer and HTS shield layers, were obtained for current distribution. In copper cryopipe about 90% of fault current flows and the copper former protect these conductor layers from burned out by over current. Moreover, the Gap-LN2 and temperature of the conductor layers were also calculated. In order to study the temperature of conductor layers and current distribution, few equivalent circuit and heat balance equations under fault current is to be formed. Gap-LN2 effect on temperature distribution of that one to four conductor layers was estimated and found that during the fault time at hP300 W/m2 K the Gap-LN2 would be completely evaporated.

Jeonwook Cho, Development and Testing of 30 m HTS Power Transmission Cable [13]

In this study, HTS power cable ,single phase 22.9kV, 30 meter long, power transmission cable have developed by Korea Electrotechnology Research Institute (KERI). In this project of efficient power transmission with zero electric loss, a HTS power transmission cable has designed, manufactured, cooled and tested experimentally. This HTS cable contains Ag/Bi-2223 tapes, insulating papers, HTS shield layers and all cooled by pressurized LN2 at temperature range of 70K to 80K. Eventually, this study portrays about the design, manufacturing, and calculation of this single phase, 30 meter long HTS power cable. It was found that the performance of HTS cable such as DC critical current (3.6 kA)

and AC loss was 0.98 W/m. In future, a planning is made to construct same length (30m) HTS cable of three phase, 50MVA.

Design and Experimental Results of a 3 Phase 30 m HTS Power Cable [14]

After developing 30 meter long HTS single phase cable, Korea Electrotechnology Research Institute (KERI) has developed the three phase 22.9kV, 50 MVA HTS power cable system. This cable contains two phase conductor layers and two layers of Ag/Bi-2223 HTS tapes and PPLP as electric insulation with LN2 as coolant. This 3 phase HTS cable tested with DC and rated current in LN2. The calculated results shows good performance of HTS cable, also proves that HTS power cable has basic electric properties for 22.9kV. Heat loss was found 3.52 W/m in u-shaped bending, 1.5 W/m in straight pipe and AC loss was 1.2kA, 77K.

Characteristics Measurements of HTS Tape with Parallel HTS Tapes [15]

To improve the AC loss properties of BSCCO and YBCO tapes, the critical currents and the transport current losses of BSCCO and YBCO tapes with paralleled magnetic material (Ni tape) and/or diamagnetic material (BSCCO tape) has investigated experimentally. With paralleled Ni tape, the critical currents of HTS tapes decreased slightly and an increment is marked in transport current losses. However, with paralleled BSCCO tape, the critical currents and transport current losses of HTS tapes have not current carrying are more improved than single HTS tape.

Both of current losses such as transport and critical current are effected by intervention of the neighboring magnetic material to an HTS tape. In order to estimate the transport current loss Norris equation is used. If the magnetism of the substrate is removed more, The AC loss of YBCO tape can be decreased.

Numerical Analysis of AC Loss Characteristics of Cable Conductor Assembled by HTS Tapes in Polygonal Arrangement [16]

In this study the AC loss characteristics of assembled conductor of multiple HTS tapes in polygonal arrangement were studied numerically with high aspect ratio. To examine the AC loss in HTS tape in polygonal arrangement a numerical model was developed in this work. The dependencies of polygonal conductor on the geometrical configuration of the AC loss characteristics such as number of tapes and gaps were verified. It was found from

the numerical results that, when YBCO tapes with high aspect ratio is used, the tape width will be lower than 3.5 mm. the gap between the tapes in polygonal arrangement should also be carefully adjusted.

Comparison of self-field effects between Bi-2223/Ag tapes and pancake coils [17]

In this present study AC losses, nature and effect of self-field in Bi-2223/Ag tape and pancake coils in terms of critical current has studied. It is proved in this work that average perpendicular component of self-field directed oppositely at the two halves of tape-width. Towards the end of tape, self-field orientation increases considerably. However, throughout the tape width for tape and single-turn coil the resultant field amplitude remains almost unchanged. Whereas, both amplitude and orientation of self-field increases toward the end of the tape for multi-turn coil. In order to develop HTS magnet or to design HTS magnet this investigation of DC and AC behavior in HTS tape and coil would be useful.

CHAPTER

4 SCOPE OF STUDY

The scope of this study is to develop the correlations for thermophysical properties of supercritical argon to be used as a coolant in HTS cable. The main advantage of using these correlations that it reduces the large number of parameters and complicated computations which helps in the modelling of HTS cable. Therefore, simulating and designing of the HTS cable with specific dimensions and materials could be done. The high temperature superconducting (HTS) cables will have the capability of transmitting high capacity current with 100% efficiency without acquiring the overhead transmission and ground space. So, the HTS cables will be the good alternative of the conventional overhead cables due to 0% A.C. losses, TW-h of produced energy can be saved. Thereby, the economy of country can be improved by saving electric energy with 100% efficiency in ways such as generating, transmitting, storing and utilizing using HTS cables.

CHAPTER

5 OBJECTIVE OF STUDY

The objectives of this thesis are:

- Selection of fluid to be used as coolant in HTS cable.
- Selection of thermophysical properties of fluid to be used as coolant.
- Study of selected thermophysical properties (specific heat, thermal conductivity, density and viscosity).
- Inspection for behavior of coolant (required more heat transfer and less pumping power)
- To develop the correlations for selected thermophysical properties of fluid to be used in HTS cable.

CHAPTER

6 RESEARCH METHODOLOGY

In this part, basically two steps are followed in order to get the critical property data. In first step, the selection of the critical thermodynamic properties such as pressure and temperature for SCAR is done by using NIST software program REFPROP [18]. Then, in order to estimate the thermophysical properties such as density, specific heat, thermal conductivity and viscosity, further NIST software program REFPROP have been used.

1.1 SELECTION OF CRITICAL PROPERTIES OF SCF

Critical temperature and pressure for SCAR is extracted from the NIST software program REFPROP [18].

Table 6-1 critical properties of supercritical Argon

Supercritical fluid	Critical temperature (K)	Critical Pressure (MPa)
SCAR	150.69	4.863

1.2 ESTIMATION OF THERMOPHYSICAL PROPERTIES OF SCF

In order to calculate the thermophysical properties such as density, heat capacity, thermal conductivity and viscosity of SCAR, NIST software program, REFPROP was applied. The program REFPROP is based on the most consistent pure fluid and mixture models currently available. REFPROP [] program was initially developed in order to estimate the refrigerant properties but further it is now extended to calculate hydrocarbon property values. The detailed information regarding this program can be found in REFPROP V7.0 []. It has a reasonable good accuracy while estimating the thermodynamic properties.

In this thesis work the statistical parameters have been used to find the accuracy of the fitted model and correlations. Small values of parameters refer to consistent correlation. Here, the Eq. (1) defines the Arithmetic Average of the Absolute Values of the Relative Errors (AARE %).

$$AARE\% = \sum_{i=1}^{500} \left(\left| \frac{X^{act} - X^{cal}}{X^{act}} \right| \right) \quad (1)$$

Table 6-2 AARE% for thermo physical properties

Properties	AARE%
Density	0.729007468
Viscosity	0.187613051
Specific heat	0.825611
Thermal Conductivity	0.811473684

The stability of correlation for concentrated data points can be stated by another parameter called Sum of Absolute of Residual (SAR) which is defined in Eq. (2).

$$SAR = \sum_{i=1}^{500} \left| X^{act} - X^{cal} \right| \quad (2)$$

Table 6-3 SAR% for thermo physical properties

Properties	SAR
Density	712.9714
Viscosity	1.6627E-05
Specific heat	7.046078
Thermal Conductivity	0.069885

Here, an extent of the predictable conclusion of the correlation given by the Average Percent Relative Error (ARE %) is defined in Eq. (3). A value of zero indicates a random of the measured values around the correlation.

$$\text{ARE}\% = \frac{100}{N} \sum_{i=1}^{500} \left(\frac{X^{act} - X^{cal}}{X^{act}} \right) \quad (3)$$

Table 6-4 ARE% for thermo physical properties

Properties	ARE%
Density	-0.2335741
Viscosity	1.32E-01
Specific heat	-0.06596
Thermal Conductivity	-0.0061487

For each thermophysical properties correlation as function of temperature, Percent Relative Error (RE %) is defined in Eq. (4)

$$RE\% = 100 \times \left(\frac{X^{act} - X^{cal}}{X^{act}}\right) \quad (4)$$

Eq. (5), expresses the standard error relation of developed correlations for higher property values as a function of temperature

$$Xerror = (X^{act} - X^{cal}) \quad (5)$$

1.3

CHAPTER

7 RESULTS AND DISCUSSIONS

7.1 STUDY OF THERMOPHYSICAL PROPERTIES

In order to understand the flow and heat transfer behavior of Supercritical Argon (SCAR), few thermophysical properties such as Density, Thermal conductivity, Viscosity, Specific heat are plotted with respect to temperature above supercritical region. Further, correlations were developed for thermophysical properties of SCAR and compared with the standard data available from NIST [13]. It is found that the deviation from the standard values is minimum as discussed in the later section.

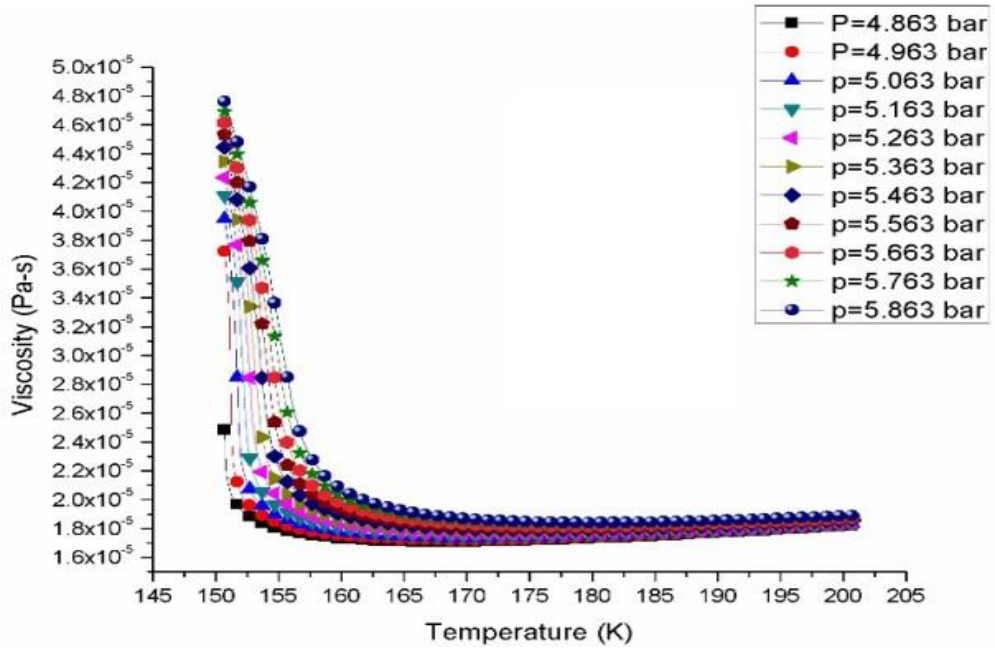

Figure 7-1 Viscosity as function of temperature at different pressures

It can be observed that with the increase in pressure, huge increase in the viscosity may be obtained in supercritical region. However, in the temperature range of 150.79K<T<165K, an initial decrease in viscosity is identified. In addition, a small increase in viscosity is observed at the end of the temperature range 165K<T<200.69K due to the increase in density as can be seen from Figure 3.

7.2 DENSITY:

Figure 7-2 shows the variation of density with temperature. In the pressure range of

48.63<P<58.63bar, extreme rise in density is observed due to the higher compression resulting in lesser intermolecular distance of the fluid. However, with in the temperature of 150.69K<T<200.69K density is regularly decreasing.

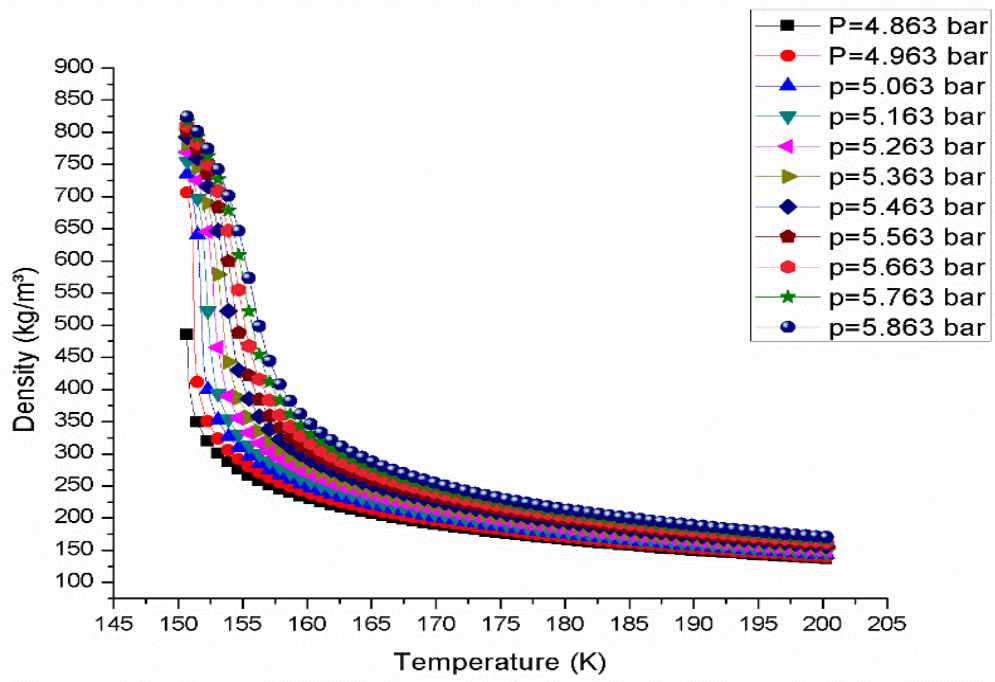

Figure 7-3 Density as function of temperature at different pressures

7.3 SPECIFIC HEAT:

Figure 7-4 shows the variation of specific heat with temperature. It can be observed that with increase in pressure from 48.63bar to 49.63bar drastic decrease in specific heat. In addition, a constant fall in specific heat with further increase in pressure from 50.63bar to 58.6bar. However, effect of temperature on specific heat results drastic decrease in the temperature range of 150.69K<T<154.89K. Furthermore, a sudden increase in the range of 154.89K<T<156.59K and then a linear fall in the range 156.59K<T<200.69K is observed.

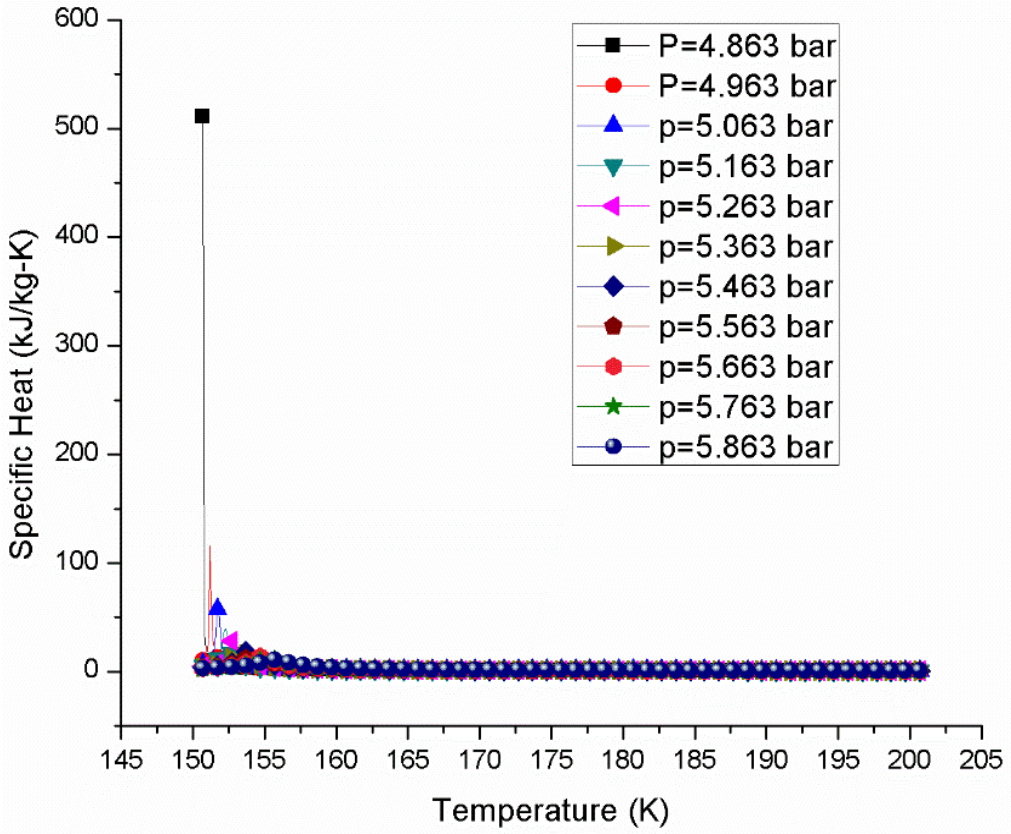

Figure 7-5 Specific Heat as function of Temperature at different pressures

7.4 THERMAL CONDUCTIVITY:

Figure 13 relates thermal conductivity as function of temperature at different pressures. The graph demonstrates significant decrease in thermal conductivity during 48.63<P<49.63bar, subsequently gradual fall is observed with further increase in pressure. However, by raise in the temperature, curves reveals uniformly diminishing values of thermal conductivity in the temperature range of 150.69

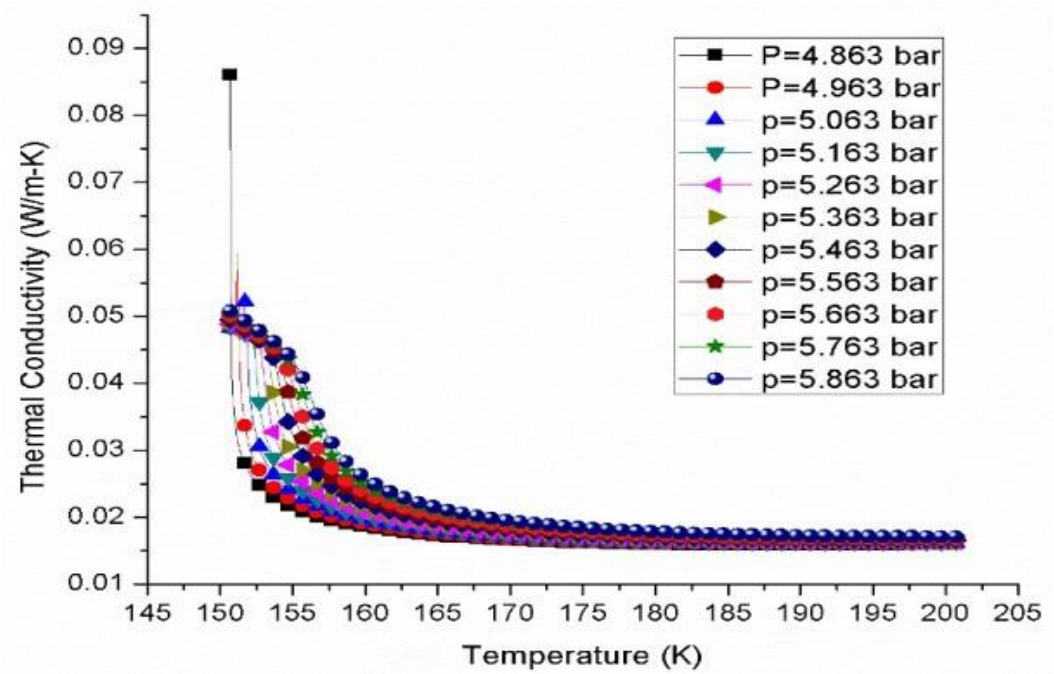

Figure 7-6 Thermal conductivity as function of Temperature at different pressures

7.6 Development of Correlations

The plots are having variation of thermophysical properties with respect temperature (T_c+50K) and Pressure (P_c+10bar) have been plotted at and above the critical point. After analyzing the plots, a drastic variation in all the thermophysical properties such as density, heat capacity, thermal conductivity and viscosity has been observed in the supercritical region. So it becomes too difficult to fit the curve with a single correlation, therefore piecewise correlations are developed in order to estimate the properties with maximum accuracy and minimum standard errors. Below are the step followed in developing correlations for the thermophysical properties of SCAR.

The correlations and the correlation coefficients obtained from fitting are compiled in Table 1. The novelty of the correlations developed [11-12] is that minimum number of c

Figure 7-7 Thermal conductivity as function of Temperature at different pressures

polynomial correlation. It is found that the developed correlations as accurate as 98% to 99% as can be seen from the Table 1.

Table 7-1 physical significance of correlation coefficients

Correlation Coefficients	**Meaning**
	Boltzmann
ρ_1, μ_1, k_1, c_{p1}	Initial Valu
ρ_2, μ_2, k_2, c_{p2}	Final Value
T	Center Value

Basically two correlations have found to estimate the values of thermophysical properties.

$$\rho = (\rho_2 + T)/(\rho_1 + \rho_3 * T) \text{---------- (1)}$$

This correlation is valid for estimation of all thermophysical properties except a temperature range 170.99 K ≤ T ≤ 200.69 K of viscosity. Due to sudden rise in viscosity of SCAR on increment in temperature.

$$\mu = (\mu_2 + \mu_3 * T)/(1+\mu_1 * T) \text{----------(2)}$$

Now this correlation is valid only for the viscosity of SCAR which is having distinct behaviour (sudden rise with increase in temperature) in a temperature range of 170.99 K ≤ T ≤ 200.69 K.

7.7 DENSITY

Density is a thermophysical property of SCAR and already discussed about the behavior as a function of temperature and presuure. In fig. 12 we can see the behavior of density as function of temperature by keeping pressure as constant. That curve is finally fitted with numerical methods and found a correlation, will be used to estimate the density of SCAR at the particular temperature by putting values in the correlation.

Table 7-2 Developed correlation for density of SCAR

Properties	Temperature Range	Correlations	Correlation Coefficient		R^2-Value
Density (ρ) (kg/m³)	150.79K ≤ T ≤ 152.59K	$\rho = (\rho_2 + T)/(\rho_1 + \rho_3 * T)$	ρ_1	-0.56814	0.99783
			ρ_2	-149.38433	
			ρ_3	0.00379	
	152.69 K ≤ T ≤ 200.69K	$\rho = (\rho_2 + T)/(\rho_1 + \rho_3 * T)$	ρ_1	-1.63179	0.99832
			ρ_2	-94.16334	
			ρ_3	0.01196	

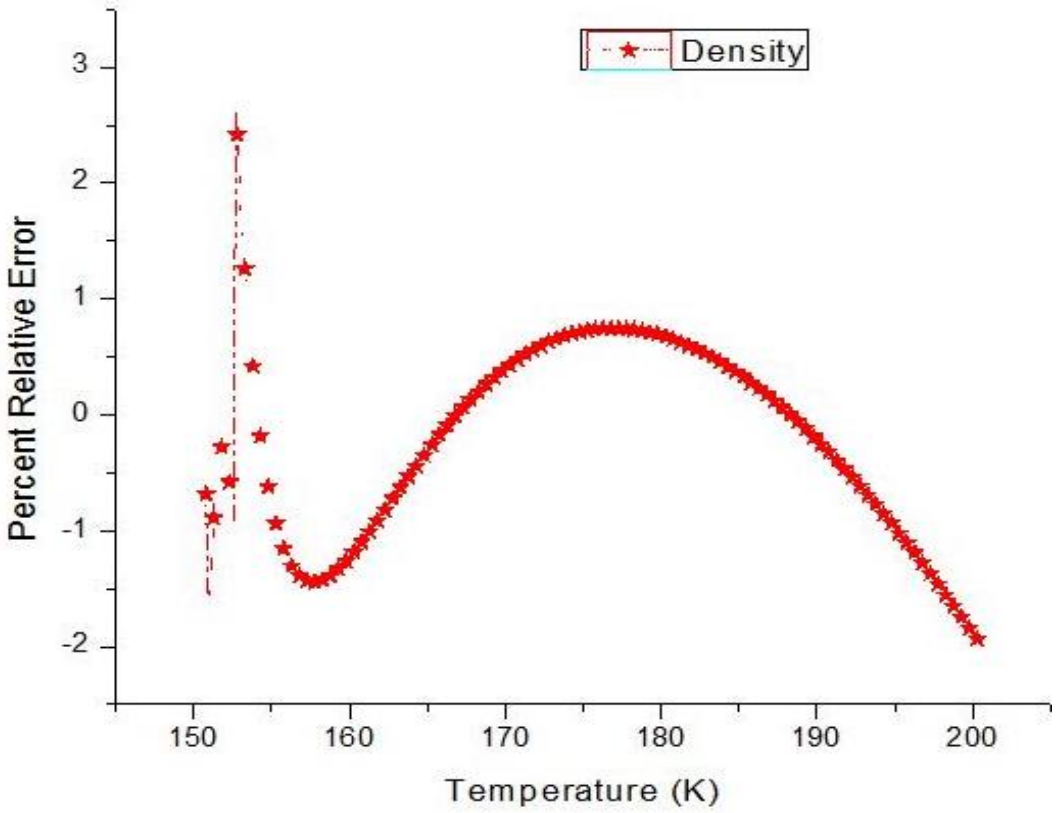

Figure 7-8 percent relative error versus temperature

The above figure shows the temperature variation on x-axis and on y-axis percent relative error. On y-axis zero (0.0) values shows the zero error, above and lower values show the error percentage of that particular property.

In this figure, it can be concluded from the graph that error for density of SCAR is having more variation just above the critical temperature (150.69K). At the end of graph can be seen, variation in error is increasing in y-axis downward direction. In the middle of graph the error is having more slope towards zero. Eventually, overall error percentage for density is 2.5%.

7.8 VISCOSITY

As viscosity is also the function of temperature and pressure shown in fig.10. The obtaining curve will be fitted to estimate a suitable range of temperature where less viscosity can be achieved at constant pressure. Now after fitting the curve few correlations are obtained same as density but for a temperature range of 170.99 K ≤ T ≤ 200.69 K, new correlation is found due to its unique behavior on increasing temperature.

Viscosity (μ) (Pa-s)	**150.79 K ≤ T ≤ 155.79 K**	$\mu = (\mu_2 + T)/(\mu_1 + \mu_3 * T)$	μ_1	**-8.81516E6**	**0.99633**
			μ_2	**-149.3863**	
			μ_3	**58884.83131**	
	150.89 K ≤ T ≤ 170.89 K	$\mu = (\mu_2 + T)/(\mu_1 + \mu_3 * T)$	μ_1	**-9.05276E6**	**0.98785**
			μ_2	**-152.46242**	
			μ_3	**59305.42314**	
	170.99 K ≤ T ≤ 200.69 K	$\mu = (\mu_2 + \mu_3 * T)/(1+\mu_1 * T)$	μ_1	**-0.00386**	**0.99905**
			μ_2	**1.55599E-5**	
			μ_3	**-5.71495E-8**	

Table 8 correlation for viscosity of SCAR

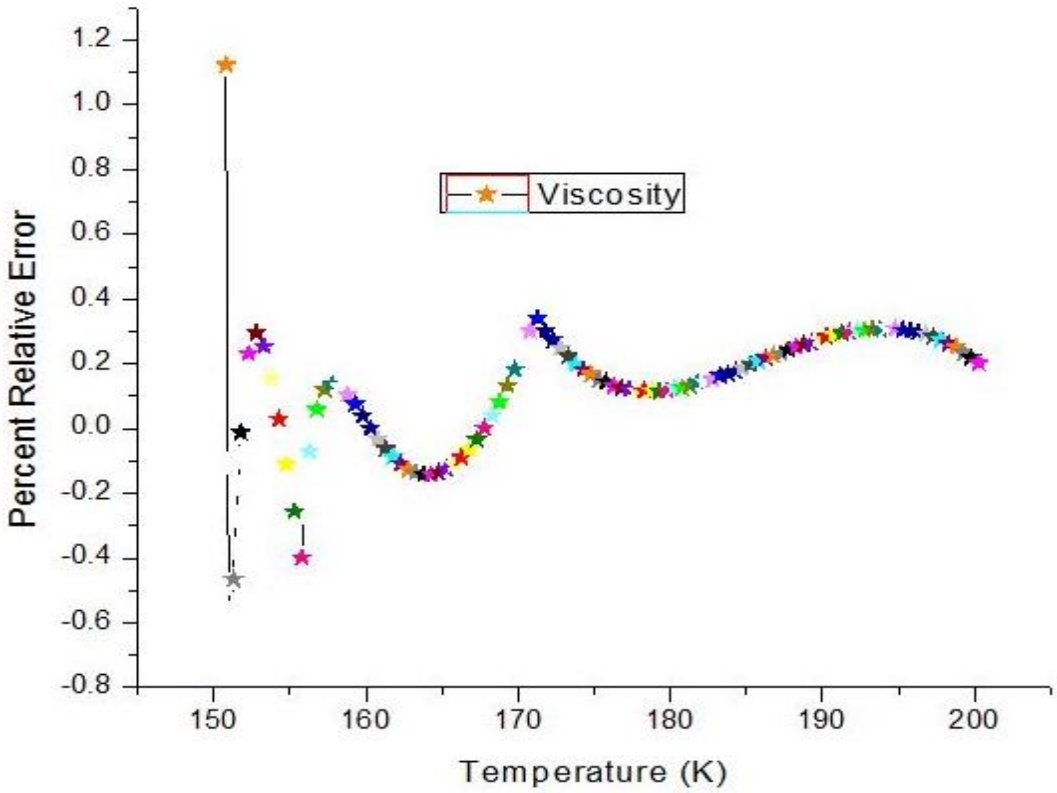

Figure 7-9 percent relative error versus temperature

The above figure shows the temperature variation on x-axis and on y-axis percent relative error. On y-axis zero (0.0) values shows the zero error, above and lower values show the error percentage of that particular property.

In this figure, it can be concluded that viscosity of SCAR is having only 1.1% relative error in the temperature range of 150.69K and just above to that temperature. On the other hand for the temperature range more than 150.69K the viscosity of SCAR is showing error less than 1% error. Now, we will see the effect of all properties in a single graph.

7.9 THERMAL CONDUCTIVITY

One of thermophysical property of SCAR is thermal conductivity and calculated as a function of temperature and pressure. By keeping pressure as constant some correlations are found using curve fitting method.

Table 9 *Developed correlation for thermal conductivity of SCAR*

Thermal Conductivity (κ) (W/m-K)	**150.79 K ≤ T ≤ 152.79K**	**$\kappa = (\kappa_2 + T)/(\kappa_1 + \kappa_3 * T)$**	**κ_1**	**-7051.18647**	**0.99639**
			κ_2	**-149.94681**	
			κ_3	**46.89732**	
	152.89 K ≤ T ≤ 200.69 K	**$\kappa = (\kappa_2 + T)/(\kappa_1 + \kappa_3 * T)$**	**κ_1**	**-10040.23758**	**0.99202**
			κ_2	**-146.17691**	
			κ_3	**67.44997**	

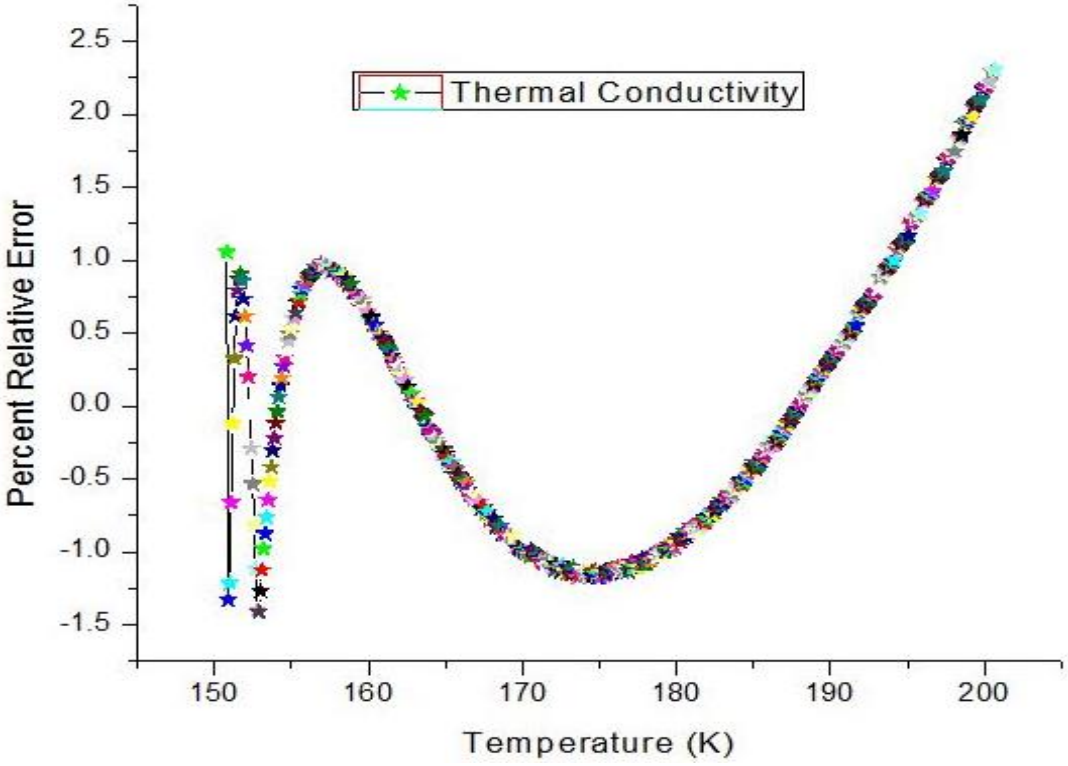

Figure 7-10 percent relative error versus temperature

The above figure shows the temperature variation on x-axis and on y-axis percent relative error. On y-axis zero (0.0) values shows the zero error, above and lower values show the error percentage of that particular property.

This figure shows that thermal conductivity of SCAR is having maximum error of 2.5% and that is at the end of the incremented temperature range 200.69K. Thermal conductivity

is having variations in the error but up to 190K, the error is very less and increasing drastically while increasing the temperature. The behavior of thermal conductivity curve is somewhat difficult to predict.

7.8. SPECIFIC HEAT

The one of transport property i.e. specific heat is calculated as a function of temperature and pressure. By keeping pressure as constant, value of specific heat is calculated in terms of temperature and can be seen in the table7. In order to estimate the heat transfer phenomenon of SCAR in HTS cable, it is needed to fit the specific heat curve. After fitting the curve a correlation is found, will help to estimate exact value of specific heat at particular temperature range.

Table 7-3 Developed correlation for specific heat of SCAR

Specific heat (c_p) (kJ/kg-K)	**150.79 K ≤ T ≤ 152.79K**	**Cp = (Cp2 +T)/(Cp1 +Cp3*T)**	**c_{p1}**	**-72.2299**	**0.99952**
			c_{p2}	**-148.33689**	
			c_{p3}	**0.47948**	
	152.89 K ≤ T ≤ 200.69 K	**Cp = (Cp2 +T)/(Cp1 +Cp3*T)**	**c_{p1}**	**-276.3881**	**0.99961**
			c_{p2}	**-128.44319**	
			c_{p3}	**1.84851**	

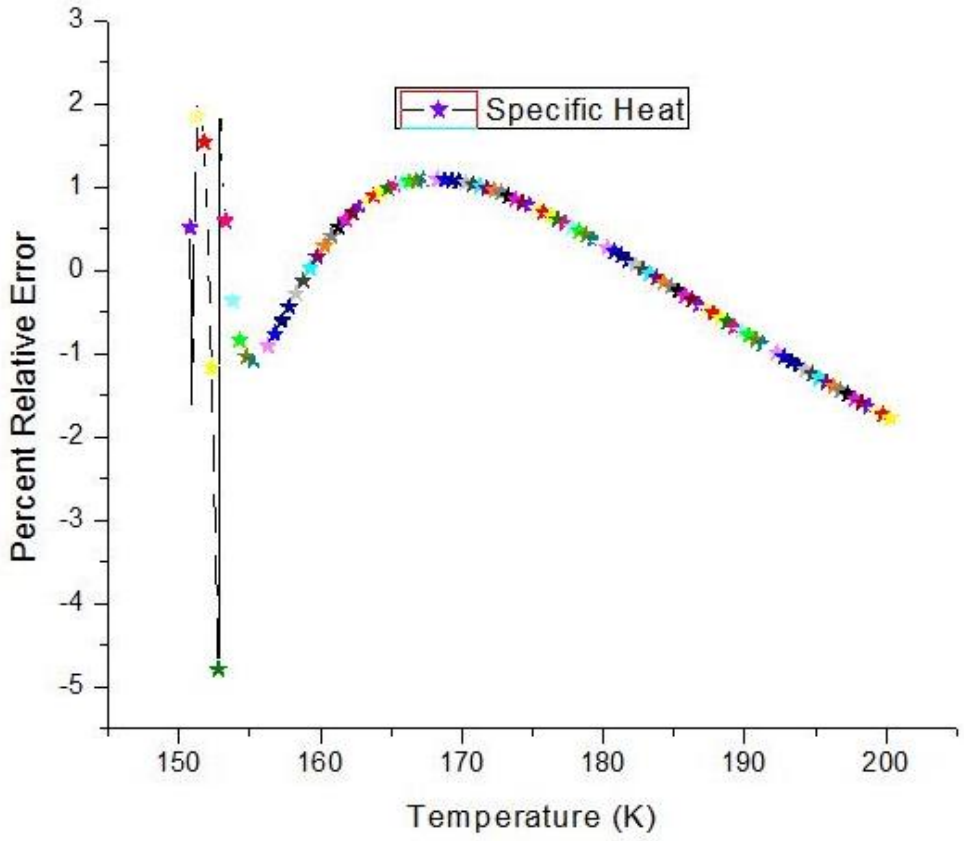

Figure 7-11 percent relative error versus temperature

The above figure shows the temperature variation on x-axis and on y-axis percent relative error. On y-axis zero (0.0) values shows the zero error, above and lower values show the error percentage of that particular property.

This figure shows that percent relative error for specific heat of SCAR is having maximum error of 5% just above the critical temperature (150.69K). The more variation is to be found near the critical point region and after the temperature range of 170K, the error is increasing drastically in y-axis downward direction. The overall error for specific heat of SCAR is 4.4% is to be observed.

7.10 RESULT OF ALL FOUR PROPERTIES

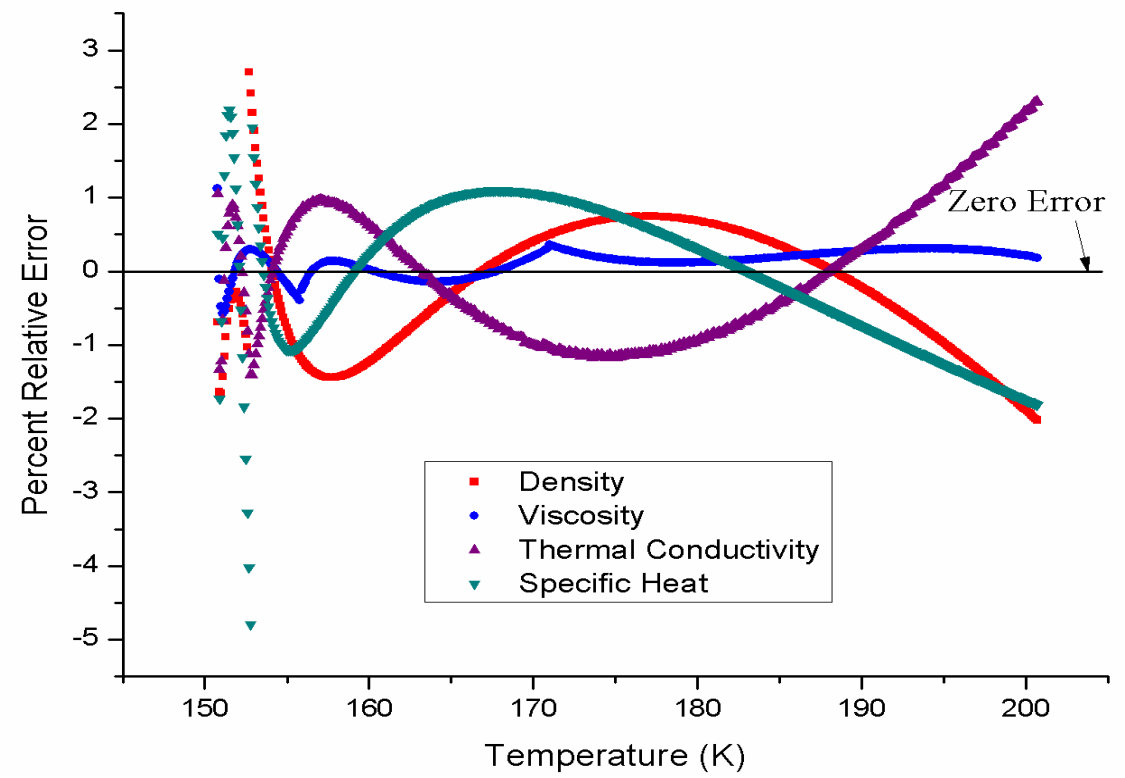

percent relative error versus temperature

The above figure shows the temperature variation on x-axis and percent relative error on y-axis with a zero error line at the zero value on y-axis. This graph is obtained with all thermophysical properties data and compiled it in a single graph. To understand the results qualitatively, a need arises to obtain this graph. In this graph all the thermophysical properties are calculated with respective percent relative errors. The performance of all properties are almost same and the value of % relative error is same too. Finally, It is concluded that only specific heat of SCAR is having more error than other three properties i.e. 5%. In order to use SCAR as coolant for high temperature superconductors, these properties will be suitable in this range.

7.9. RESULTS WITH CFD APPROACH

In this study, some results has been developed using CFD (computational fluid dynamics) approach. CFD is used to predict the fluid flow (transport phenomenon) behavior using conservation equations. To compute this problem, FLUENT 6.3.26 software has been used.

A geometry of 1 meter HTS cable is modelled and meshed in GAMBIT 2.2.30, then imported to fluent 6.3.26. In fluent post processing part was done using some assumptions and periodic boundary conditions. In order to predict the internal behavior of SCAR, some simulations were performed. As the fluid flow was compressible and turbulent, some turbulence models have used and validated in this work. Two different turbulence models have used in the present work.

1. k - ω std (k-omega standard)
2. k - ω sst (k-omega sst)

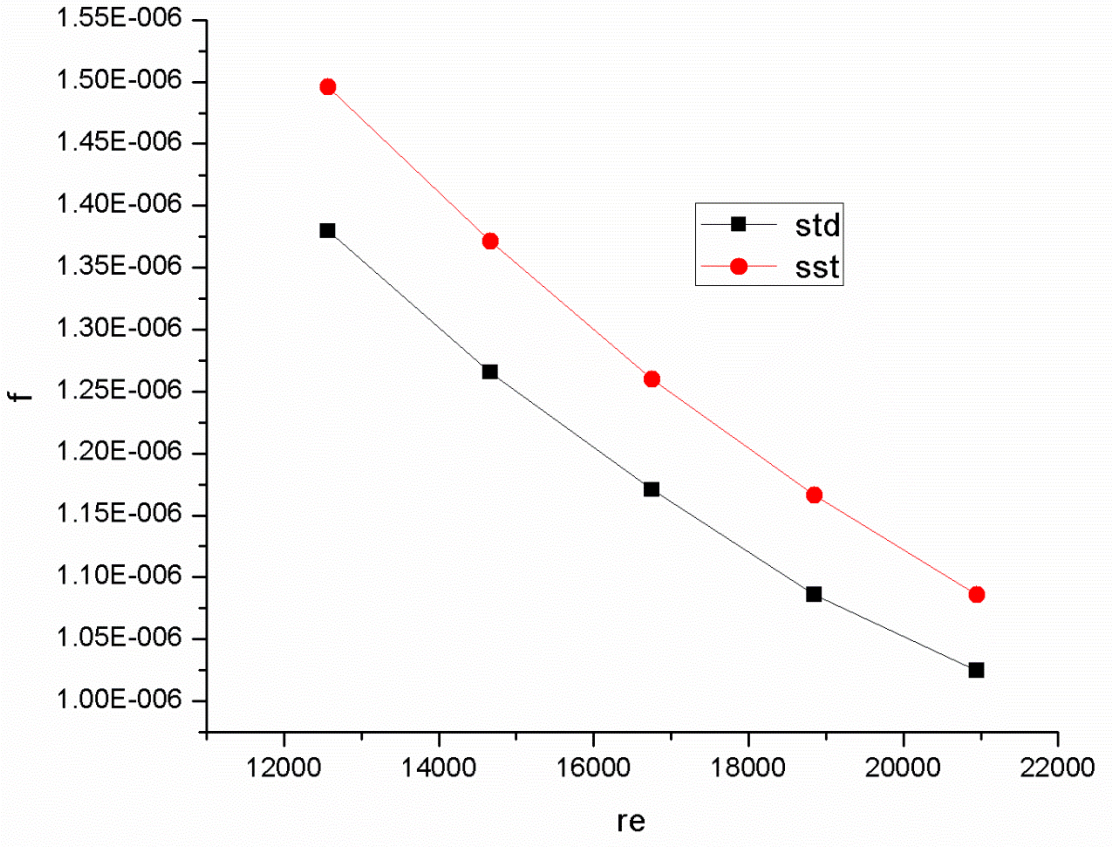

Figure 0-1Reynolds number vs friction factor

This figure shows a relation between Reynolds number (x-axis) and friction factor (y-axis) of both the turbulence model for the different heat transfer in leaks.

In order to get the suitable correlation, this Re versus f curve has fitted in polynomial order.

The obtained correlations are:

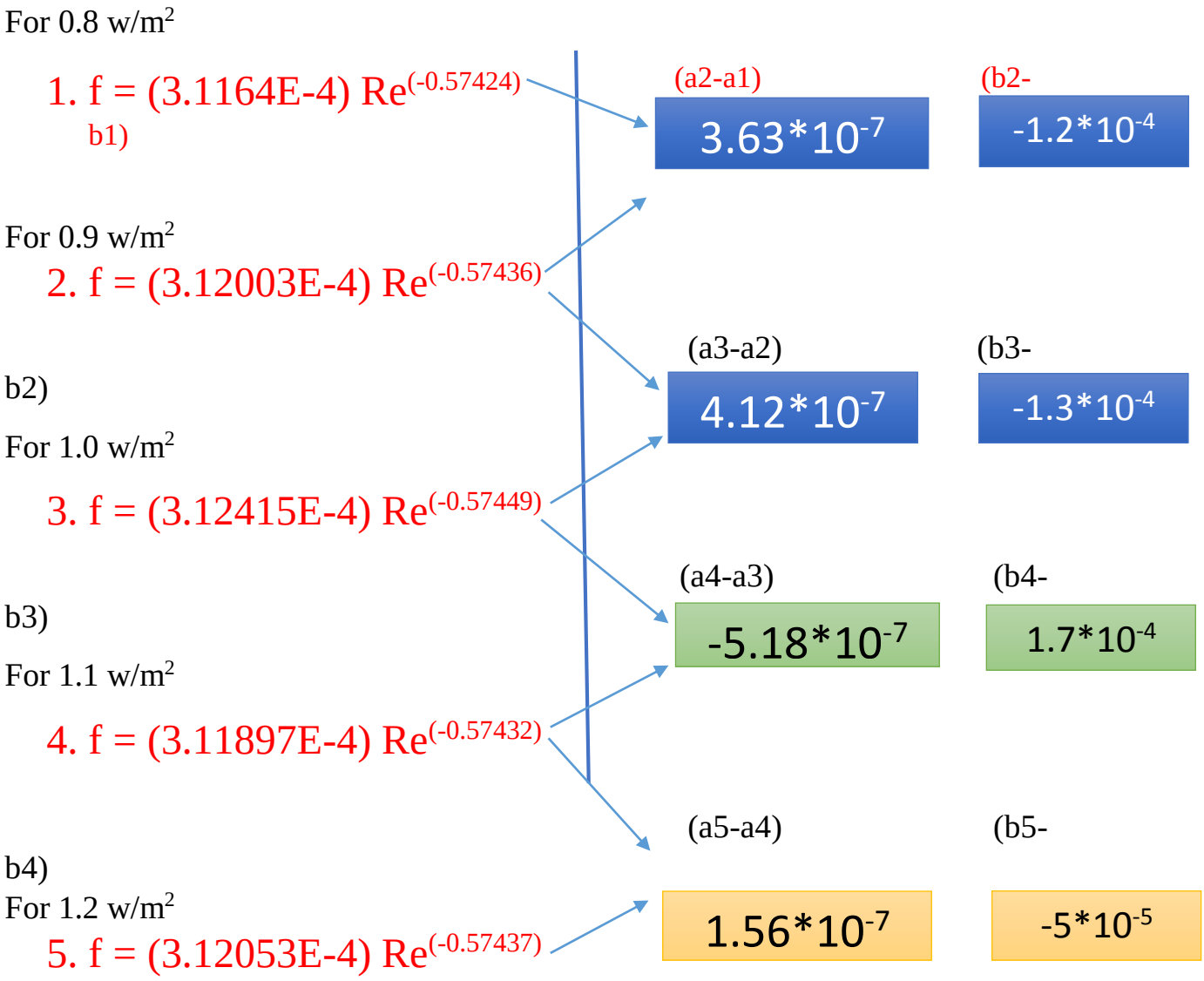

This chart shows the different correlations for different heat in leaks from ambient to coolant. F stands for friction factor and Re stands for Reynolds number. For 1st correlation a1, a2, b1, b2 are the constant terms of Re and f. Similarly, other correlations are having different constants and the difference of constants on right side is very less. Finally, due to very less

difference in constants a correlation can be make global correlation.

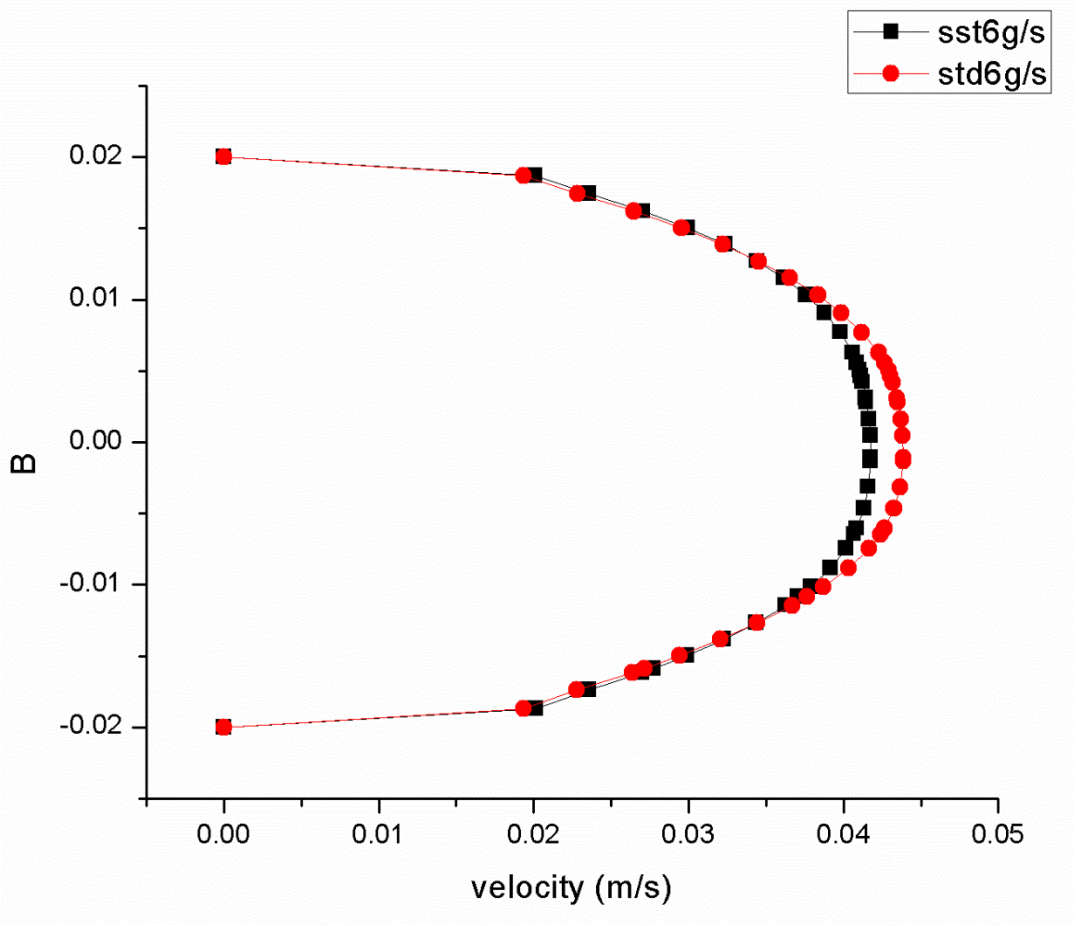

Figure 21 velocity profile vs diameter

This figure shows the developed velocity profile of SCAR in the former pipe of HTS cable. The mass flow rate of fluid was 6g/s for both turbulence models. The velocity profile was developed at 0.04m/s for 40mm diameter pipe using k-ω sst and on the other hand velocity profile developed at 0.045m/s for k-ω std.

CHAPTER

8. CONCLUSIONS AND FUTURE SCOPE

8.1. SUMMARY AND CONCLUSION

In this thesis work an explanation has been given about the Superconductors, HTS cable and Supercritical fluid. Thus, an attempt has been made to develop the correlation for the thermophysical properties such as density, viscosity, thermal conductivity and specific heat of SCAR for the development of HTS cable using high temperature superconductors such as Hg based having critical temperature up to 134K. Since, SCAR is having critical temperature of 150.69K, so it can be used only for the Hg based superconductors, which are going to be manufactured. As fig. _ shows that the superconductors up to 240K has been discovered. However, due to the complications in design, manufacturing of these superconductors is still in process.

It is concluded that In order to calculate accurately various thermophysical properties, the correlations are being proposed in this work and the developed correlation were compared with standard data from NIST [13]. Moreover, the thermophysical properties of supercritical Argon portrays interesting facts on pressure and temperature distribution in HTS cable. This work also explains the phenomenon of flow occurrence with less pumping power and maximum heat transfer through coolant in HTS cables.

It can be concluded that in the temperature range of $195K<T<200.69K$ at $P=4.963bar$, the density of SCAR would be minimum. However, the viscosity of SCAR is expected less value in the temperature range of $157.5K<T<172.5K$ at $P=4.963$ bar above the supercritical region. Moreover, this study would help in continuous flow of coolant with minimum pumping power.

In order to increase the heat transfer, higher value of specific heat of SCAR is needed at $P=5.063bar$ in the temperature range of $151K<T<152.5K$. However, the thermal conductivity of SCAR is expected higher value at $P=5.063$ bar in the temperature range of $150.79K<T<155K$.

8.2. FUTURE SCOPE

In the regard of future scope, study of correlation development and thermophysical properties of SCAR will be helpful in designing and simulating HTS cable. Moreover, this study will predicted that SCAR may be the most suitable coolant for high temperature superconductors i.e. Hg based. These developed correlations for thermophysical properties is the function of temperature and pressure, that will tell the exact temperature & pressure range, where SCAR would have more heat transfer and less pumping power for the cooling of HTS cable. The main advantage of using developed correlations is that it does not required any large number of parameters and complicated computations.

In addition, the study of thermophysical properties such as density, viscosity, thermal conductivity and specific heat will describe the behavior of SCAR. In other words the maximum heat transfer and less pumping power can be achieved by the study of correlations for thermophysical properties of SCAR. Thus, these correlations will contribute an innovative HTS cable design to this world for the efficient power transmission.

References

[1] R Wesche, A Anghel, B Jakob, G Pasztor, R Schindler, G Vécsey, Design of superconducting power cables, Cryogenics, Volume 39, Issue 9, 1 September 1999, Pages 767-775

[2] Jin-Wook Choi; Jae-Hyeong Choi; Hae-Jong Kim; Jeonwook Cho; Sang-Hyun Kim, Manufacture and insulating test of a mini-model for 154 kV-class HTS cables, Applied Superconductivity, IEEE Transactions on , vol.19, no.3, pp.1789,1792, June 2009

[3] Azad Jarrahian, Ehsan Heidaryan, A novel correlation approach to estimate thermal conductivity of pure carbon dioxide in the supercritical region, The Journal of Supercritical Fluids, Volume 64, April 2012, Pages 39-45

[4] Ali Akbar Amooey, A simple correlation to predict thermal conductivity of supercritical carbon dioxide, The Journal of Supercritical Fluids, Volume 86, February 2014, Pages 1-3

[5] P. Zhang, Y. Huang, B. Shen, R.Z. Wang, Flow and heat transfer characteristics of supercritical nitrogen in a vertical mini-tube, International Journal of Thermal Sciences, Volume 50, Issue 3, March 2011, Pages 287-295

[6] Jin-Hong, Joo, Seog-Whan Kim, Hae Joon Kim, Kyu Jeong Song, and Jung-Pyo Hong, Design of HTS tape characteristics measurement system, Applied Superconductivity, IEEE Transactions on, vol.14, no.2, June 2004

[7] Jeonwook cho, Ki-Chul Seong, Kang-Sik Ryu, A design and tests of HTS power cables and feasibility study of HTS power transmission system in Korea, Applied Superconductivity, IEEE Transactions on, vol.10, no.1, March 2000

[8] Seungyon Cho, Seung-Hyun Kim, Dong-Lak Kim, Ki-Hak Im, HyungSuk Yang, Do-Hyeong Kim, and Won-Moog Jung, Calculation of alternating current distribution on the current lead for HTS power cable, Applied Superconductivity, IEEE, transactions on, vol.14, no.2, June 2004

[9] Ehsan Heidaryana ,Azad Jarrahian, Modified Redlich–Kwong equation of state for supercritical carbon dioxide, supercritical fluids, 81 (2013) 92– 98

[10] Dondapati, R.S.; Rao, V.V., "Pressure Drop and Heat Transfer Analysis of Long Length Internally Cooled HTS Cables, "Applied Superconductivity, IEEE Transactions on, vol.23, no.3, pp.5400604, 5400604, June 2013.

[11] A. Sasaki, Yu. Ivanov, S. Yamaguchi,"LN2 circulation in cryopipes of superconducting power transmission line, Cryogenics, volume 51, 14 May 2011, pages 471–476.

[12] J. Fang , H.F. Li , J.H. Zhu , Z.N. Zhou , Y.X. Li , Z. Shen , D.L. Dong , T. Yu, Z.M. Li , M. Qiu, Numerical analysis of the stability of HTS power cable under fault current considering the gaps in the cable, Physica C, volume 494, 19 april 2013, pages 319–323.

[13] Jeonwook Cho, Joon-Han Bae, Hae-Jong Kim, Ki-Deok Sim, Ki-Chul Seong, Hyun-Man Jang, and Dong-Wook Kim, Development and Testing of 30 m HTS Power Transmission Cable, Applied Superconductivity, IEEE Transactions on, vol. 15, on. 2, JUNE 2005

[14] Jeonwook Cho, Ki-Deok Sim, Joon-Han Bae, Hae-Jong Kim, Jae-Ho Kim, Ki-Chul Seong, Hyun-Man Jang, Chang-Young Lee, and Deuk-Yong Koh, Design and Experimental Results of a 3 Phase 30 m HTS Power Cable, Applied Superconductivity, IEEE Transactions on, vol. 16, no. 2, June 2006

[15] Jin-Hong Joo, Seog-Whan Kim, Kyu Jeong Song, Chan Park, Rock-Kil Ko, Ho-Sup Kim, Jung-Pyo Hong, and SeokBeom Kim, Characteristics Measurements of HTS Tape with Parallel HTS Tapes, Applied Superconductivity, IEEE Transactions on, vol. 16, no. 2, June 2006

[16] Satoshi Fukui, Ryuichi Kojima, Jun Ogawa, Mitsugi Yamaguchi, Takao Sato, and Osami Tsukamoto, Numerical Analysis of AC Loss Characteristics of Cable Conductor Assembled by HTS Tapes in Polygonal Arrangement, IEEE Transactions on, vol. 16, no. 2, June 2006

[17] A.K.M. Alamgir *, C. Gu, Z. Han, Comparison of self-field effects between Bi-2223/Ag tapes and pancake coils, Physica C, volume 424, 19 april 2013, pages 138–144, May 2005

[18] E.W. Lemmon, M.L. Huber, M.O. McLinden, NIST Standard Reference Database 23: Reference Fluid Thermodynamic and Transport Properties – REFPROP, Version 9.0, 2010.

APPENDIX

Temperature	Pressure	Density	Cp	Therm. Cond.	Viscosity
(K)	(MPa)	(kg/m³)	(kJ/kg-K)	(W/m-K)	(Pa-s)
150.69	4.863	484.83	511.11	0.08601	2.4829E-5
150.79	4.863	416.24	34.783	0.04165	2.215E-5
150.89	4.863	396.83	21.119	0.03701	2.1468E-5
150.99	4.863	384.11	15.8	0.03454	2.1039E-5
151.09	4.863	374.43	12.88	0.03289	2.0722E-5
151.19	4.863	366.54	11.005	0.03166	2.047E-5
151.29	4.863	359.83	9.6851	0.03069	2.026E-5
151.39	4.863	353.97	8.6989	0.02988	2.008E-5
151.49	4.863	348.76	7.9302	0.02919	1.9923E-5
151.59	4.863	344.05	7.3115	0.02859	1.9784E-5
151.69	4.863	339.76	6.8014	0.02807	1.9658E-5
151.79	4.863	335.8	6.3724	0.0276	1.9545E-5
151.89	4.863	332.13	6.0058	0.02717	1.944E-5
151.99	4.863	328.7	5.6884	0.02679	1.9345E-5
152.09	4.863	325.49	5.4104	0.02643	1.9256E-5
152.19	4.863	322.46	5.1647	0.0261	1.9173E-5
152.29	4.863	319.6	4.9456	0.0258	1.9096E-5
152.39	4.863	316.88	4.7489	0.02551	1.9023E-5
152.49	4.863	314.29	4.5711	0.02525	1.8955E-5
152.59	4.863	311.82	4.4095	0.025	1.8891E-5
152.69	4.863	309.46	4.2619	0.02476	1.883E-5
152.79	4.863	307.19	4.1264	0.02454	1.8772E-5
152.89	4.863	305.02	4.0016	0.02432	1.8717E-5
152.99	4.863	302.93	3.8862	0.02412	1.8665E-5
153.09	4.863	300.91	3.7791	0.02393	1.8615E-5

153.19	4.863	298.97	3.6793	0.02375	1.8568E-5
153.29	4.863	297.09	3.5862	0.02357	1.8522E-5
153.39	4.863	295.27	3.499	0.0234	1.8479E-5
153.49	4.863	293.5	3.4173	0.02324	1.8437E-5
153.59	4.863	291.79	3.3403	0.02309	1.8397E-5
153.69	4.863	290.14	3.2678	0.02294	1.8358E-5
153.79	4.863	288.52	3.1993	0.0228	1.8321E-5
153.89	4.863	286.96	3.1346	0.02266	1.8286E-5
153.99	4.863	285.43	3.0732	0.02253	1.8251E-5
154.09	4.863	283.94	3.0149	0.0224	1.8218E-5
154.19	4.863	282.5	2.9595	0.02228	1.8186E-5
154.29	4.863	281.08	2.9067	0.02216	1.8155E-5
154.39	4.863	279.7	2.8564	0.02204	1.8125E-5
154.49	4.863	278.36	2.8084	0.02193	1.8096E-5
154.59	4.863	277.04	2.7625	0.02182	1.8068E-5
154.69	4.863	275.76	2.7186	0.02171	1.8041E-5
154.79	4.863	274.5	2.6765	0.02161	1.8015E-5
154.89	4.863	273.26	2.6362	0.02151	1.7989E-5
154.99	4.863	272.06	2.5974	0.02141	1.7965E-5
155.09	4.863	270.88	2.5602	0.02132	1.7941E-5
155.19	4.863	269.72	2.5245	0.02122	1.7918E-5
155.29	4.863	268.58	2.49	0.02113	1.7895E-5
155.39	4.863	267.47	2.4569	0.02105	1.7873E-5
155.49	4.863	266.37	2.4249	0.02096	1.7852E-5
155.59	4.863	265.3	2.394	0.02088	1.7831E-5
155.69	4.863	264.25	2.3642	0.0208	1.7811E-5
155.79	4.863	263.21	2.3355	0.02072	1.7791E-5
155.89	4.863	262.19	2.3077	0.02064	1.7772E-5
155.99	4.863	261.19	2.2807	0.02057	1.7754E-5
156.09	4.863	260.21	2.2547	0.02049	1.7735E-5

156.19	4.863	259.24	2.2295	0.02042	1.7718E-5
156.29	4.863	258.29	2.205	0.02035	1.7701E-5
156.39	4.863	257.36	2.1813	0.02028	1.7684E-5
156.49	4.863	256.43	2.1583	0.02021	1.7668E-5
156.59	4.863	255.53	2.136	0.02015	1.7652E-5
156.69	4.863	254.63	2.1143	0.02008	1.7636E-5
156.79	4.863	253.75	2.0932	0.02002	1.7621E-5
156.89	4.863	252.88	2.0728	0.01996	1.7607E-5
156.99	4.863	252.03	2.0528	0.0199	1.7592E-5
157.09	4.863	251.19	2.0335	0.01984	1.7578E-5
157.19	4.863	250.36	2.0146	0.01978	1.7565E-5
157.29	4.863	249.54	1.9962	0.01972	1.7551E-5
157.39	4.863	248.73	1.9783	0.01966	1.7538E-5
157.49	4.863	247.93	1.9609	0.01961	1.7526E-5
157.59	4.863	247.14	1.9439	0.01955	1.7513E-5
157.69	4.863	246.37	1.9273	0.0195	1.7501E-5
157.79	4.863	245.6	1.9112	0.01945	1.7489E-5
157.89	4.863	244.84	1.8954	0.0194	1.7478E-5
157.99	4.863	244.1	1.88	0.01935	1.7467E-5
158.09	4.863	243.36	1.8649	0.0193	1.7455E-5
158.19	4.863	242.63	1.8502	0.01925	1.7445E-5
158.29	4.863	241.91	1.8359	0.0192	1.7434E-5
158.39	4.863	241.2	1.8218	0.01916	1.7424E-5
158.49	4.863	240.5	1.8081	0.01911	1.7414E-5
158.59	4.863	239.8	1.7947	0.01907	1.7404E-5
158.69	4.863	239.11	1.7816	0.01902	1.7395E-5
158.79	4.863	238.43	1.7687	0.01898	1.7385E-5
158.89	4.863	237.76	1.7561	0.01894	1.7376E-5
158.99	4.863	237.1	1.7438	0.01889	1.7367E-5
159.09	4.863	236.44	1.7318	0.01885	1.7359E-5

159.19	4.863	235.79	1.72	0.01881	1.735E-5
159.29	4.863	235.15	1.7084	0.01877	1.7342E-5
159.39	4.863	234.52	1.697	0.01873	1.7334E-5
159.49	4.863	233.89	1.6859	0.01869	1.7326E-5
159.59	4.863	233.27	1.675	0.01866	1.7318E-5
159.69	4.863	232.65	1.6643	0.01862	1.731E-5
159.79	4.863	232.04	1.6538	0.01858	1.7303E-5
159.89	4.863	231.44	1.6436	0.01854	1.7296E-5
159.99	4.863	230.84	1.6335	0.01851	1.7288E-5
160.09	4.863	230.25	1.6235	0.01847	1.7282E-5
160.19	4.863	229.66	1.6138	0.01844	1.7275E-5
160.29	4.863	229.08	1.6043	0.0184	1.7268E-5
160.39	4.863	228.51	1.5949	0.01837	1.7262E-5
160.49	4.863	227.94	1.5857	0.01834	1.7255E-5
160.59	4.863	227.38	1.5766	0.0183	1.7249E-5
160.69	4.863	226.82	1.5677	0.01827	1.7243E-5
160.79	4.863	226.27	1.559	0.01824	1.7237E-5
160.89	4.863	225.72	1.5504	0.01821	1.7232E-5
160.99	4.863	225.18	1.542	0.01818	1.7226E-5
161.09	4.863	224.64	1.5337	0.01815	1.7221E-5
161.19	4.863	224.11	1.5255	0.01812	1.7215E-5
161.29	4.863	223.58	1.5175	0.01809	1.721E-5
161.39	4.863	223.06	1.5096	0.01806	1.7205E-5
161.49	4.863	222.54	1.5018	0.01803	1.72E-5
161.59	4.863	222.02	1.4941	0.018	1.7195E-5
161.69	4.863	221.51	1.4866	0.01797	1.7191E-5
161.79	4.863	221.01	1.4792	0.01794	1.7186E-5
161.89	4.863	220.51	1.4719	0.01792	1.7182E-5
161.99	4.863	220.01	1.4647	0.01789	1.7177E-5
162.09	4.863	219.52	1.4577	0.01786	1.7173E-5

162.19	4.863	219.03	1.4507	0.01784	1.7169E-5
162.29	4.863	218.54	1.4438	0.01781	1.7165E-5
162.39	4.863	218.06	1.4371	0.01779	1.7161E-5
162.49	4.863	217.58	1.4304	0.01776	1.7157E-5
162.59	4.863	217.11	1.4239	0.01774	1.7153E-5
162.69	4.863	216.64	1.4174	0.01771	1.715E-5
162.79	4.863	216.18	1.411	0.01769	1.7146E-5
162.89	4.863	215.71	1.4048	0.01766	1.7143E-5
162.99	4.863	215.25	1.3986	0.01764	1.7139E-5
163.09	4.863	214.8	1.3925	0.01762	1.7136E-5
163.19	4.863	214.35	1.3865	0.0176	1.7133E-5
163.29	4.863	213.9	1.3805	0.01757	1.713E-5
163.39	4.863	213.45	1.3747	0.01755	1.7127E-5
163.49	4.863	213.01	1.3689	0.01753	1.7124E-5
163.59	4.863	212.58	1.3632	0.01751	1.7121E-5
163.69	4.863	212.14	1.3576	0.01749	1.7118E-5
163.79	4.863	211.71	1.3521	0.01746	1.7116E-5
163.89	4.863	211.28	1.3466	0.01744	1.7113E-5
163.99	4.863	210.85	1.3412	0.01742	1.7111E-5
164.09	4.863	210.43	1.3359	0.0174	1.7108E-5
164.19	4.863	210.01	1.3306	0.01738	1.7106E-5
164.29	4.863	209.59	1.3254	0.01736	1.7104E-5
164.39	4.863	209.18	1.3203	0.01734	1.7102E-5
164.49	4.863	208.77	1.3152	0.01732	1.71E-5
164.59	4.863	208.36	1.3103	0.0173	1.7098E-5
164.69	4.863	207.96	1.3053	0.01728	1.7096E-5
164.79	4.863	207.55	1.3005	0.01726	1.7094E-5
164.89	4.863	207.16	1.2956	0.01725	1.7092E-5
164.99	4.863	206.76	1.2909	0.01723	1.709E-5
165.09	4.863	206.36	1.2862	0.01721	1.7089E-5

165.19	4.863	205.97	1.2816	0.01719	1.7087E-5
165.29	4.863	205.58	1.277	0.01717	1.7086E-5
165.39	4.863	205.2	1.2725	0.01716	1.7084E-5
165.49	4.863	204.81	1.268	0.01714	1.7083E-5
165.59	4.863	204.43	1.2636	0.01712	1.7081E-5
165.69	4.863	204.05	1.2592	0.01711	1.708E-5
165.79	4.863	203.68	1.2549	0.01709	1.7079E-5
165.89	4.863	203.3	1.2506	0.01707	1.7078E-5
165.99	4.863	202.93	1.2464	0.01706	1.7077E-5
166.09	4.863	202.56	1.2422	0.01704	1.7076E-5
166.19	4.863	202.19	1.2381	0.01703	1.7075E-5
166.29	4.863	201.83	1.234	0.01701	1.7074E-5
166.39	4.863	201.47	1.23	0.017	1.7073E-5
166.49	4.863	201.1	1.226	0.01698	1.7072E-5
166.59	4.863	200.75	1.2221	0.01696	1.7071E-5
166.69	4.863	200.39	1.2182	0.01695	1.7071E-5
166.79	4.863	200.04	1.2143	0.01693	1.707E-5
166.89	4.863	199.68	1.2105	0.01692	1.707E-5
166.99	4.863	199.34	1.2067	0.01691	1.7069E-5
167.09	4.863	198.99	1.203	0.01689	1.7069E-5
167.19	4.863	198.64	1.1993	0.01688	1.7068E-5
167.29	4.863	198.3	1.1957	0.01686	1.7068E-5
167.39	4.863	197.96	1.192	0.01685	1.7068E-5
167.49	4.863	197.62	1.1885	0.01684	1.7067E-5
167.59	4.863	197.28	1.1849	0.01682	1.7067E-5
167.69	4.863	196.94	1.1814	0.01681	1.7067E-5
167.79	4.863	196.61	1.178	0.0168	1.7067E-5
167.89	4.863	196.28	1.1745	0.01678	1.7067E-5
167.99	4.863	195.95	1.1711	0.01677	1.7067E-5
168.09	4.863	195.62	1.1678	0.01676	1.7067E-5

168.19	4.863	195.29	1.1644	0.01675	1.7067E-5
168.29	4.863	194.97	1.1611	0.01673	1.7067E-5
168.39	4.863	194.65	1.1579	0.01672	1.7067E-5
168.49	4.863	194.33	1.1546	0.01671	1.7067E-5
168.59	4.863	194.01	1.1514	0.0167	1.7068E-5
168.69	4.863	193.69	1.1483	0.01668	1.7068E-5
168.79	4.863	193.38	1.1451	0.01667	1.7068E-5
168.89	4.863	193.06	1.142	0.01666	1.7069E-5
168.99	4.863	192.75	1.139	0.01665	1.7069E-5
169.09	4.863	192.44	1.1359	0.01664	1.707E-5
169.19	4.863	192.13	1.1329	0.01663	1.707E-5
169.29	4.863	191.82	1.1299	0.01662	1.7071E-5
169.39	4.863	191.52	1.127	0.01661	1.7071E-5
169.49	4.863	191.21	1.124	0.01659	1.7072E-5
169.59	4.863	190.91	1.1211	0.01658	1.7073E-5
169.69	4.863	190.61	1.1182	0.01657	1.7073E-5
169.79	4.863	190.31	1.1154	0.01656	1.7074E-5
169.89	4.863	190.01	1.1126	0.01655	1.7075E-5
169.99	4.863	189.72	1.1098	0.01654	1.7076E-5
170.09	4.863	189.42	1.107	0.01653	1.7076E-5
170.19	4.863	189.13	1.1042	0.01652	1.7077E-5
170.29	4.863	188.84	1.1015	0.01651	1.7078E-5
170.39	4.863	188.55	1.0988	0.0165	1.7079E-5
170.49	4.863	188.26	1.0961	0.01649	1.708E-5
170.59	4.863	187.97	1.0935	0.01649	1.7081E-5
170.69	4.863	187.68	1.0909	0.01648	1.7082E-5
170.79	4.863	187.4	1.0883	0.01647	1.7084E-5
170.89	4.863	187.12	1.0857	0.01646	1.7085E-5
170.99	4.863	186.83	1.0831	0.01645	1.7086E-5
171.09	4.863	186.55	1.0806	0.01644	1.7087E-5

171.19	4.863	186.28	1.0781	0.01643	1.7088E-5
171.29	4.863	186	1.0756	0.01642	1.709E-5
171.39	4.863	185.72	1.0731	0.01641	1.7091E-5
171.49	4.863	185.45	1.0706	0.0164	1.7092E-5
171.59	4.863	185.17	1.0682	0.0164	1.7094E-5
171.69	4.863	184.9	1.0658	0.01639	1.7095E-5
171.79	4.863	184.63	1.0634	0.01638	1.7096E-5
171.89	4.863	184.36	1.061	0.01637	1.7098E-5
171.99	4.863	184.09	1.0587	0.01636	1.7099E-5
172.09	4.863	183.82	1.0564	0.01635	1.7101E-5
172.19	4.863	183.56	1.054	0.01635	1.7103E-5
172.29	4.863	183.29	1.0518	0.01634	1.7104E-5
172.39	4.863	183.03	1.0495	0.01633	1.7106E-5
172.49	4.863	182.77	1.0472	0.01632	1.7107E-5
172.59	4.863	182.5	1.045	0.01632	1.7109E-5
172.69	4.863	182.24	1.0428	0.01631	1.7111E-5
172.79	4.863	181.99	1.0406	0.0163	1.7113E-5
172.89	4.863	181.73	1.0384	0.01629	1.7114E-5
172.99	4.863	181.47	1.0362	0.01629	1.7116E-5
173.09	4.863	181.22	1.0341	0.01628	1.7118E-5
173.19	4.863	180.96	1.0319	0.01627	1.712E-5
173.29	4.863	180.71	1.0298	0.01627	1.7122E-5
173.39	4.863	180.46	1.0277	0.01626	1.7124E-5
173.49	4.863	180.21	1.0256	0.01625	1.7125E-5
173.59	4.863	179.96	1.0236	0.01624	1.7127E-5
173.69	4.863	179.71	1.0215	0.01624	1.7129E-5
173.79	4.863	179.46	1.0195	0.01623	1.7131E-5
173.89	4.863	179.21	1.0175	0.01623	1.7133E-5
173.99	4.863	178.97	1.0155	0.01622	1.7135E-5
174.09	4.863	178.72	1.0135	0.01621	1.7138E-5

174.19	4.863	178.48	1.0115	0.01621	1.714E-5
174.29	4.863	178.24	1.0095	0.0162	1.7142E-5
174.39	4.863	178	1.0076	0.01619	1.7144E-5
174.49	4.863	177.76	1.0057	0.01619	1.7146E-5
174.59	4.863	177.52	1.0038	0.01618	1.7148E-5
174.69	4.863	177.28	1.0019	0.01618	1.7151E-5
174.79	4.863	177.04	0.99998	0.01617	1.7153E-5
174.89	4.863	176.8	0.9981	0.01616	1.7155E-5
174.99	4.863	176.57	0.99625	0.01616	1.7157E-5
175.09	4.863	176.34	0.9944	0.01615	1.716E-5
175.19	4.863	176.1	0.99257	0.01615	1.7162E-5
175.29	4.863	175.87	0.99075	0.01614	1.7164E-5
175.39	4.863	175.64	0.98895	0.01614	1.7167E-5
175.49	4.863	175.41	0.98715	0.01613	1.7169E-5
175.59	4.863	175.18	0.98537	0.01613	1.7172E-5
175.69	4.863	174.95	0.98361	0.01612	1.7174E-5
175.79	4.863	174.72	0.98185	0.01612	1.7177E-5
175.89	4.863	174.49	0.98011	0.01611	1.7179E-5
175.99	4.863	174.27	0.97838	0.01611	1.7182E-5
176.09	4.863	174.04	0.97667	0.0161	1.7184E-5
176.19	4.863	173.82	0.97496	0.0161	1.7187E-5
176.29	4.863	173.6	0.97327	0.01609	1.7189E-5
176.39	4.863	173.37	0.97159	0.01609	1.7192E-5
176.49	4.863	173.15	0.96992	0.01608	1.7194E-5
176.59	4.863	172.93	0.96826	0.01608	1.7197E-5
176.69	4.863	172.71	0.96661	0.01607	1.72E-5
176.79	4.863	172.49	0.96498	0.01607	1.7202E-5
176.89	4.863	172.28	0.96335	0.01606	1.7205E-5
176.99	4.863	172.06	0.96174	0.01606	1.7208E-5
177.09	4.863	171.84	0.96014	0.01606	1.7211E-5

177.19	4.863	171.63	0.95855	0.01605	1.7213E-5
177.29	4.863	171.41	0.95696	0.01605	1.7216E-5
177.39	4.863	171.2	0.95539	0.01604	1.7219E-5
177.49	4.863	170.98	0.95384	0.01604	1.7222E-5
177.59	4.863	170.77	0.95229	0.01603	1.7225E-5
177.69	4.863	170.56	0.95075	0.01603	1.7227E-5
177.79	4.863	170.35	0.94922	0.01603	1.723E-5
177.89	4.863	170.14	0.9477	0.01602	1.7233E-5
177.99	4.863	169.93	0.94619	0.01602	1.7236E-5
178.09	4.863	169.72	0.94469	0.01601	1.7239E-5
178.19	4.863	169.52	0.9432	0.01601	1.7242E-5
178.29	4.863	169.31	0.94172	0.01601	1.7245E-5
178.39	4.863	169.1	0.94025	0.016	1.7248E-5
178.49	4.863	168.9	0.93879	0.016	1.7251E-5
178.59	4.863	168.69	0.93734	0.016	1.7254E-5
178.69	4.863	168.49	0.9359	0.01599	1.7257E-5
178.79	4.863	168.29	0.93447	0.01599	1.726E-5
178.89	4.863	168.08	0.93305	0.01599	1.7263E-5
178.99	4.863	167.88	0.93163	0.01598	1.7266E-5
179.09	4.863	167.68	0.93023	0.01598	1.7269E-5
179.19	4.863	167.48	0.92883	0.01598	1.7272E-5
179.29	4.863	167.28	0.92744	0.01597	1.7275E-5
179.39	4.863	167.08	0.92606	0.01597	1.7279E-5
179.49	4.863	166.89	0.92469	0.01597	1.7282E-5
179.59	4.863	166.69	0.92333	0.01596	1.7285E-5
179.69	4.863	166.49	0.92198	0.01596	1.7288E-5
179.79	4.863	166.3	0.92063	0.01596	1.7291E-5
179.89	4.863	166.1	0.9193	0.01595	1.7295E-5
179.99	4.863	165.91	0.91797	0.01595	1.7298E-5
180.09	4.863	165.71	0.91665	0.01595	1.7301E-5

180.19	4.863	165.52	0.91534	0.01595	1.7304E-5
180.29	4.863	165.33	0.91403	0.01594	1.7308E-5
180.39	4.863	165.14	0.91274	0.01594	1.7311E-5
180.49	4.863	164.94	0.91145	0.01594	1.7314E-5
180.59	4.863	164.75	0.91017	0.01594	1.7318E-5
180.69	4.863	164.56	0.90889	0.01593	1.7321E-5
180.79	4.863	164.38	0.90763	0.01593	1.7324E-5
180.89	4.863	164.19	0.90637	0.01593	1.7328E-5
180.99	4.863	164	0.90512	0.01593	1.7331E-5
181.09	4.863	163.81	0.90388	0.01592	1.7334E-5
181.19	4.863	163.63	0.90264	0.01592	1.7338E-5
181.29	4.863	163.44	0.90141	0.01592	1.7341E-5
181.39	4.863	163.25	0.90019	0.01591	1.7345E-5
181.49	4.863	163.07	0.89898	0.01591	1.7348E-5
181.59	4.863	162.89	0.89777	0.01591	1.7352E-5
181.69	4.863	162.7	0.89657	0.01591	1.7355E-5
181.79	4.863	162.52	0.89538	0.01591	1.7359E-5
181.89	4.863	162.34	0.8942	0.0159	1.7362E-5
181.99	4.863	162.15	0.89302	0.0159	1.7366E-5
182.09	4.863	161.97	0.89184	0.0159	1.7369E-5
182.19	4.863	161.79	0.89068	0.0159	1.7373E-5
182.29	4.863	161.61	0.88952	0.0159	1.7376E-5
182.39	4.863	161.43	0.88837	0.01589	1.738E-5
182.49	4.863	161.26	0.88722	0.01589	1.7383E-5
182.59	4.863	161.08	0.88608	0.01589	1.7387E-5
182.69	4.863	160.9	0.88495	0.01589	1.7391E-5
182.79	4.863	160.72	0.88382	0.01589	1.7394E-5
182.89	4.863	160.55	0.8827	0.01589	1.7398E-5
182.99	4.863	160.37	0.88159	0.01588	1.7402E-5
183.09	4.863	160.2	0.88048	0.01588	1.7405E-5

183.19	4.863	160.02	0.87938	0.01588	1.7409E-5
183.29	4.863	159.85	0.87829	0.01588	1.7413E-5
183.39	4.863	159.67	0.8772	0.01588	1.7416E-5
183.49	4.863	159.5	0.87612	0.01588	1.742E-5
183.59	4.863	159.33	0.87504	0.01587	1.7424E-5
183.69	4.863	159.16	0.87397	0.01587	1.7427E-5
183.79	4.863	158.98	0.8729	0.01587	1.7431E-5
183.89	4.863	158.81	0.87184	0.01587	1.7435E-5
183.99	4.863	158.64	0.87079	0.01587	1.7439E-5
184.09	4.863	158.47	0.86974	0.01587	1.7443E-5
184.19	4.863	158.3	0.8687	0.01587	1.7446E-5
184.29	4.863	158.13	0.86766	0.01586	1.745E-5
184.39	4.863	157.97	0.86663	0.01586	1.7454E-5
184.49	4.863	157.8	0.86561	0.01586	1.7458E-5
184.59	4.863	157.63	0.86459	0.01586	1.7462E-5
184.69	4.863	157.47	0.86357	0.01586	1.7465E-5
184.79	4.863	157.3	0.86256	0.01586	1.7469E-5
184.89	4.863	157.13	0.86156	0.01586	1.7473E-5
184.99	4.863	156.97	0.86056	0.01586	1.7477E-5
185.09	4.863	156.8	0.85957	0.01586	1.7481E-5
185.19	4.863	156.64	0.85858	0.01585	1.7485E-5
185.29	4.863	156.48	0.8576	0.01585	1.7489E-5
185.39	4.863	156.31	0.85662	0.01585	1.7493E-5
185.49	4.863	156.15	0.85565	0.01585	1.7497E-5
185.59	4.863	155.99	0.85468	0.01585	1.7501E-5
185.69	4.863	155.83	0.85372	0.01585	1.7505E-5
185.79	4.863	155.66	0.85276	0.01585	1.7509E-5
185.89	4.863	155.5	0.85181	0.01585	1.7513E-5
185.99	4.863	155.34	0.85086	0.01585	1.7517E-5
186.09	4.863	155.18	0.84992	0.01585	1.7521E-5

186.19	4.863	155.02	0.84898	0.01585	1.7525E-5
186.29	4.863	154.87	0.84805	0.01585	1.7529E-5
186.39	4.863	154.71	0.84712	0.01584	1.7533E-5
186.49	4.863	154.55	0.8462	0.01584	1.7537E-5
186.59	4.863	154.39	0.84528	0.01584	1.7541E-5
186.69	4.863	154.23	0.84437	0.01584	1.7545E-5
186.79	4.863	154.08	0.84346	0.01584	1.7549E-5
186.89	4.863	153.92	0.84255	0.01584	1.7553E-5
186.99	4.863	153.77	0.84165	0.01584	1.7557E-5
187.09	4.863	153.61	0.84076	0.01584	1.7561E-5
187.19	4.863	153.46	0.83987	0.01584	1.7565E-5
187.29	4.863	153.3	0.83898	0.01584	1.7569E-5
187.39	4.863	153.15	0.8381	0.01584	1.7573E-5
187.49	4.863	153	0.83722	0.01584	1.7578E-5
187.59	4.863	152.84	0.83635	0.01584	1.7582E-5
187.69	4.863	152.69	0.83548	0.01584	1.7586E-5
187.79	4.863	152.54	0.83461	0.01584	1.759E-5
187.89	4.863	152.39	0.83375	0.01584	1.7594E-5
187.99	4.863	152.23	0.83289	0.01584	1.7598E-5
188.09	4.863	152.08	0.83204	0.01584	1.7603E-5
188.19	4.863	151.93	0.83119	0.01584	1.7607E-5
188.29	4.863	151.78	0.83035	0.01584	1.7611E-5
188.39	4.863	151.63	0.82951	0.01584	1.7615E-5
188.49	4.863	151.48	0.82867	0.01584	1.7619E-5
188.59	4.863	151.34	0.82784	0.01584	1.7624E-5
188.69	4.863	151.19	0.82702	0.01584	1.7628E-5
188.79	4.863	151.04	0.82619	0.01584	1.7632E-5
188.89	4.863	150.89	0.82537	0.01584	1.7636E-5
188.99	4.863	150.75	0.82456	0.01584	1.7641E-5
189.09	4.863	150.6	0.82374	0.01584	1.7645E-5

189.19	4.863	150.45	0.82294	0.01584	1.7649E-5
189.29	4.863	150.31	0.82213	0.01584	1.7653E-5
189.39	4.863	150.16	0.82133	0.01584	1.7658E-5
189.49	4.863	150.02	0.82053	0.01584	1.7662E-5
189.59	4.863	149.87	0.81974	0.01584	1.7666E-5
189.69	4.863	149.73	0.81895	0.01584	1.7671E-5
189.79	4.863	149.58	0.81817	0.01584	1.7675E-5
189.89	4.863	149.44	0.81739	0.01584	1.7679E-5
189.99	4.863	149.3	0.81661	0.01584	1.7684E-5
190.09	4.863	149.15	0.81583	0.01584	1.7688E-5
190.19	4.863	149.01	0.81506	0.01584	1.7692E-5
190.29	4.863	148.87	0.81429	0.01584	1.7697E-5
190.39	4.863	148.73	0.81353	0.01584	1.7701E-5
190.49	4.863	148.59	0.81277	0.01584	1.7706E-5
190.59	4.863	148.45	0.81201	0.01584	1.771E-5
190.69	4.863	148.31	0.81126	0.01584	1.7714E-5
190.79	4.863	148.17	0.81051	0.01584	1.7719E-5
190.89	4.863	148.03	0.80977	0.01584	1.7723E-5
190.99	4.863	147.89	0.80902	0.01584	1.7728E-5
191.09	4.863	147.75	0.80828	0.01584	1.7732E-5
191.19	4.863	147.61	0.80755	0.01584	1.7736E-5
191.29	4.863	147.47	0.80681	0.01584	1.7741E-5
191.39	4.863	147.33	0.80608	0.01584	1.7745E-5
191.49	4.863	147.19	0.80536	0.01584	1.775E-5
191.59	4.863	147.06	0.80464	0.01584	1.7754E-5
191.69	4.863	146.92	0.80392	0.01584	1.7759E-5
191.79	4.863	146.78	0.8032	0.01585	1.7763E-5
191.89	4.863	146.65	0.80249	0.01585	1.7768E-5
191.99	4.863	146.51	0.80178	0.01585	1.7772E-5
192.09	4.863	146.38	0.80107	0.01585	1.7777E-5

192.19	4.863	146.24	0.80037	0.01585	1.7781E-5
192.29	4.863	146.11	0.79967	0.01585	1.7786E-5
192.39	4.863	145.97	0.79897	0.01585	1.779E-5
192.49	4.863	145.84	0.79827	0.01585	1.7795E-5
192.59	4.863	145.71	0.79758	0.01585	1.7799E-5
192.69	4.863	145.57	0.79689	0.01585	1.7804E-5
192.79	4.863	145.44	0.79621	0.01585	1.7808E-5
192.89	4.863	145.31	0.79553	0.01585	1.7813E-5
192.99	4.863	145.17	0.79485	0.01585	1.7818E-5
193.09	4.863	145.04	0.79417	0.01585	1.7822E-5
193.19	4.863	144.91	0.7935	0.01586	1.7827E-5
193.29	4.863	144.78	0.79283	0.01586	1.7831E-5
193.39	4.863	144.65	0.79216	0.01586	1.7836E-5
193.49	4.863	144.52	0.7915	0.01586	1.7841E-5
193.59	4.863	144.39	0.79083	0.01586	1.7845E-5
193.69	4.863	144.26	0.79017	0.01586	1.785E-5
193.79	4.863	144.13	0.78952	0.01586	1.7854E-5
193.89	4.863	144	0.78887	0.01586	1.7859E-5
193.99	4.863	143.87	0.78822	0.01586	1.7864E-5
194.09	4.863	143.74	0.78757	0.01586	1.7868E-5
194.19	4.863	143.61	0.78692	0.01586	1.7873E-5
194.29	4.863	143.48	0.78628	0.01587	1.7878E-5
194.39	4.863	143.36	0.78564	0.01587	1.7882E-5
194.49	4.863	143.23	0.785	0.01587	1.7887E-5
194.59	4.863	143.1	0.78437	0.01587	1.7892E-5
194.69	4.863	142.97	0.78374	0.01587	1.7896E-5
194.79	4.863	142.85	0.78311	0.01587	1.7901E-5
194.89	4.863	142.72	0.78248	0.01587	1.7906E-5
194.99	4.863	142.6	0.78186	0.01587	1.791E-5
195.09	4.863	142.47	0.78124	0.01587	1.7915E-5

195.19	4.863	142.34	0.78062	0.01588	1.792E-5
195.29	4.863	142.22	0.78001	0.01588	1.7924E-5
195.39	4.863	142.09	0.77939	0.01588	1.7929E-5
195.49	4.863	141.97	0.77878	0.01588	1.7934E-5
195.59	4.863	141.85	0.77817	0.01588	1.7938E-5
195.69	4.863	141.72	0.77757	0.01588	1.7943E-5
195.79	4.863	141.6	0.77697	0.01588	1.7948E-5
195.89	4.863	141.48	0.77637	0.01588	1.7953E-5
195.99	4.863	141.35	0.77577	0.01589	1.7957E-5
196.09	4.863	141.23	0.77517	0.01589	1.7962E-5
196.19	4.863	141.11	0.77458	0.01589	1.7967E-5
196.29	4.863	140.99	0.77399	0.01589	1.7972E-5
196.39	4.863	140.86	0.7734	0.01589	1.7977E-5
196.49	4.863	140.74	0.77281	0.01589	1.7981E-5
196.59	4.863	140.62	0.77223	0.01589	1.7986E-5
196.69	4.863	140.5	0.77165	0.01589	1.7991E-5
196.79	4.863	140.38	0.77107	0.0159	1.7996E-5
196.89	4.863	140.26	0.77049	0.0159	1.8E-5
196.99	4.863	140.14	0.76992	0.0159	1.8005E-5
197.09	4.863	140.02	0.76935	0.0159	1.801E-5
197.19	4.863	139.9	0.76878	0.0159	1.8015E-5
197.29	4.863	139.78	0.76821	0.0159	1.802E-5
197.39	4.863	139.66	0.76765	0.0159	1.8025E-5
197.49	4.863	139.54	0.76708	0.01591	1.8029E-5
197.59	4.863	139.42	0.76652	0.01591	1.8034E-5
197.69	4.863	139.31	0.76596	0.01591	1.8039E-5
197.79	4.863	139.19	0.76541	0.01591	1.8044E-5
197.89	4.863	139.07	0.76485	0.01591	1.8049E-5
197.99	4.863	138.95	0.7643	0.01591	1.8054E-5
198.09	4.863	138.84	0.76375	0.01591	1.8058E-5

198.19	4.863	138.72	0.7632	0.01592	1.8063E-5
198.29	4.863	138.6	0.76266	0.01592	1.8068E-5
198.39	4.863	138.49	0.76212	0.01592	1.8073E-5
198.49	4.863	138.37	0.76158	0.01592	1.8078E-5
198.59	4.863	138.25	0.76104	0.01592	1.8083E-5
198.69	4.863	138.14	0.7605	0.01593	1.8088E-5
198.79	4.863	138.02	0.75996	0.01593	1.8093E-5
198.89	4.863	137.91	0.75943	0.01593	1.8097E-5
198.99	4.863	137.79	0.7589	0.01593	1.8102E-5
199.09	4.863	137.68	0.75837	0.01593	1.8107E-5
199.19	4.863	137.56	0.75785	0.01593	1.8112E-5
199.29	4.863	137.45	0.75732	0.01594	1.8117E-5
199.39	4.863	137.34	0.7568	0.01594	1.8122E-5
199.49	4.863	137.22	0.75628	0.01594	1.8127E-5
199.59	4.863	137.11	0.75576	0.01594	1.8132E-5
199.69	4.863	137	0.75524	0.01594	1.8137E-5
199.79	4.863	136.88	0.75473	0.01594	1.8142E-5
199.89	4.863	136.77	0.75422	0.01595	1.8147E-5
199.99	4.863	136.66	0.75371	0.01595	1.8152E-5
200.09	4.863	136.55	0.7532	0.01595	1.8157E-5
200.19	4.863	136.44	0.75269	0.01595	1.8162E-5
200.29	4.863	136.33	0.75219	0.01595	1.8167E-5
200.39	4.863	136.21	0.75168	0.01595	1.8172E-5
200.49	4.863	136.1	0.75118	0.01596	1.8176E-5
200.59	4.863	135.99	0.75068	0.01596	1.8181E-5
200.69	4.863	135.88	0.75019	0.01596	1.8186E-5

Table of Content

LIST OF FIGURES

LIST OF TABLES